Title: Mapping neuronal gene expression reveals aspects of ganglionic organization in a gastropod mollusc

Authors: Ramirez MD, Bui TN, and Katz PS
Department of Biology
University of Massachusetts Amherst

Abstract (348 words)

Gastropod molluscs, such as *Aplysia*, *Lymnaea*, and *Tritonia* have been important for determining fundamental rules of motor control and learning and memory because they have individually identifiable neurons. This has allowed neural circuits to be worked out using pair-wise microelectrode recordings. However, neuronal identification that relies on electrophysiology, dye tracing, and immunohistochemistry, limits research to the small number of large neurons, ignoring the much larger number of small neurons. Here we combined high throughput, single-cell RNA sequencing (scRNAseq) with *in situ* hybridization chain reaction (HCR) to examine gene expression in the head ganglia of the gastropod, *Berghia stephanieae*. Cluster analysis of the transcriptomic data uncovered multiple neuronal cell clusters, as well as glial, fibroblast, and endothelial cell clusters in the central ring ganglia (CRG: cerebral, pleural, pedal, and buccal ganglia) and the rhinophore ganglia (*rhg*). Combinatorial molecular signatures were layered on top of size and position using HCR with multiplexed marker genes to help establish specific neuronal class and type phenotypes. Unannotated genes made up significant proportions of the top differentially expressed genes for each cluster, including the most ubiquitously expressed pan-neuronal marker. Neuronal classes expressing major neurotransmitter phenotypes of glutamatergic, cholinergic, and serotonergic neurons were

identified. Some neurons co-expressed genes for two neurotransmitters. Serotonergic neurons, not cholinergic neurons, were found to express *Unc-4*. Among the neurons found to be glutamatergic were a single photoreceptor in the eye and *Soluble guanylate cyclase* (*Sgc*)-expressing neurons in the *rhg*. A sampling of expression patterns from 8 out of the 40 molluscan neuropeptides identified in the single-cell dataset showed the tremendous diversity of neuron types, with few neuropeptides co-expressed in the same neurons. A visually identifiable giant ventral neuron was found to express three peptides and *Chat*. A subset of neurons in *rhg*, which contain only small somata (<15 μm), separated into three clusters: 1) glutamatergic + *Sgc* neurons, 2) nitric oxide synthase (*Nos*) + pigment dispersing factor (*Pdf*), and 3) *Nos/Pdf-*. The three groups were spatially restricted in the *rhg*. Transcription factors marked a cluster of newly differentiated neurons and were expressed in mature neurons. *Six3/6* was expressed only in neurons from the rhinophore and cerebral ganglia, which are anterior-most of the major head ganglia, consistent with *Six3/6* anterior segregation in other animals. This study provides the foundation for understanding the fundamental neuronal organization of the gastropod nervous system.

Introduction

The central nervous system (CNS) including the brain contains many different cell types, forming the basis of its complex structure and connectivity, and allowing it to perform sophisticated functions. The diversity of cell types in CNS is reflected in differential gene expression across neurons (Lein et al. 2007; Vergara et al. 2017). Analysis of high-throughput single cell RNA sequencing (scRNAseq) allows classification of neurons based on gene expression across the entire CNS (Brunet Avalos et al. 2019; Styfhals et al. 2022). The central ring ganglia (CRG) of gastropod molluscs, such as *Aplysia, Tritonia,* and *Lymnaea* contain large individually identifiable neurons that have allowed their clear classification based on immunohistochemistry (IHC), neuroanatomy, and neurophysiology (Katz and Quinlan 2019; Leonard 2000). These same characteristics can be used to identify homologous neurons across species (Roger P. Croll 1987; James M. Newcomb et al. 2012). However, this approach is limited to the small number of large neurons that are impaleable with intracellular microelectrodes. Moreover, this approach is limited by the availability of antisera that reliably label antigens without cross-reactivity and does not easily scale up to the thousands of small neurons in the CRG or smaller neurons in other ganglia. Here, we combine scRNAseq with *in* situ hybridization chain reaction (HCR) to obtain a more complete atlas of neurons in head ganglia of the gastropod, *Berghia stephanieae* (Fig. 1). Creating neuron type profiles that incorporate visualization of multiplexed marker genes as well as other neuronal features such as soma size and position should enable the identification of neuronal sub-classes and even individual cell types in gastropods, as has been done in well-studied laboratory species like *C. elegans* and *Drosophila melanogaster*.

Berghia offers many advantages over other standardly used gastropods for high throughput neuroscience research. First, it has a 2-month generation time and can be reared and raised in

the lab with minimal effort. It is also available from commercial aquarium vendors. Like other nudibranchs, the CRG, consisting of the cerebral ganglion (*ceg*), pleural ganglion (*plg*), pedal ganglion (*pdg*), and buccal ganglion (*bcg*), are condensed in the head (Fig 1B, C). As we will show, homologs of neurons that have been identified in other species can be found in *Berghia* (Whitesel 2021; Watkins 2022).

There are challenges for high throughput scRNAseq in gastropods. First, there is a ten-fold variation in soma size, with the smallest neurons being less than 10 microns and the largest over 100 microns in diameter. CRG have fewer than 10,000 neurons overall, limiting the number of neurons that could be obtained from each sample for sequencing. Many of the largest neurons are fragile and not able to withstand some protocols for cell dissociation. Finally, many neurons are represented as a single bilateral pair per animal. Thus, obtaining the numbers of neurons typically used in scRNAseq studies is unfeasible.

In addition to the CRG, gastropods have ganglia associated with various peripheral organs, such as the genitals, tentacles, and rhinophores. In most nudibranchs, the rhinophore ganglion (*rhg*) is located distally within the rhinophore, an appendage used for distance chemoreception (Arey 1918; Cummins and Wyeth 2014; Storch and Welsch 1969; Wertz et al. 2006). However, in *Berghia* the *rhg* sits at the base of the rhinophore and is separated from the CRG by a short nerve connective. Unlike neurons in the CRG, no individual neurons or clusters have been identified in the *rhg*, due primarily to the small size of the neurons and their inaccessibility to standard methods for identifying neurons in gastropods. The combination of scRNAseq and HCR offers an opportunity to catalog these peripheral neurons.

The results presented here describe neuronal gene expression in the CRG and *rhg*, showing that multiple neuronal classes, as well as non-neuronal cell types, can be recognized by

differential gene expression. Other specific neuron types can be identified using combinations of gene expression, soma size and position information. While orthologs of neuronal genes known from other phyla are useful, we found that unknown, unannotated genes represented a surprisingly sizable proportion of cluster-specific markers, highlighting that unannotated genes should not be disregarded when using creating gene expression profiles for cell types, especially in understudied phyla like molluscs. We also present results showing unexpected diversity and organization of the neurons in the *rhg*, which suggest a high degree of complexity in this peripheral ganglion. This study highlights the use of modern, high-throughput molecular methods to develop a gene-based atlas of neurons in non-traditional study species.

Results

Single cell isolation and sequencing

To obtain single cell sequences, neurons were dissociated from the head ganglia of 20 healthy adult *Berghia stephanieae* and sequenced. Ganglia were dissected out of the head. The *rhg* were separated from the CRG by cutting the nerve connective between them (Fig. 1B). The *rhg* and CRG samples required separate processing due to differences in the average size of neurons in each sample. Most neurons in the *rhg* were less than 10μm in diameter, whereas CRG neurons ranged from 10-60μm in diameter (Fig 1C). After digestion, cells were dissociated using gentle agitation, filtered, fixed in methanol and then stored at -20°C while additional samples were collected. Single neuron libraries were prepared using 10X Genomics and sequenced on an Illumina NovaSeq.

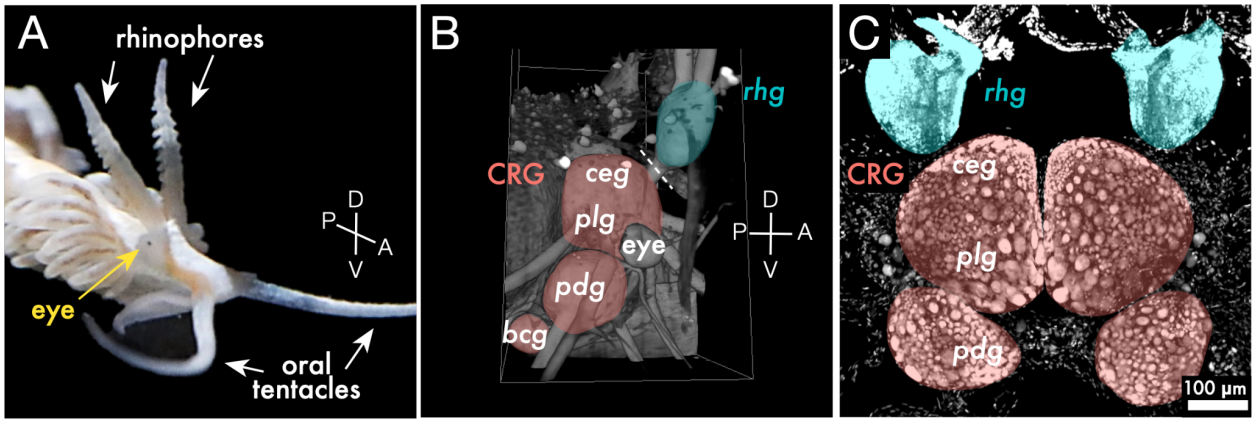

Figure 1: The *Berghia* brain atlas consists of cells taken from the central ring ganglia (CRG) and rhinophore ganglia. A) An adult *Berghia stephanieae*, showing the head and positions of the rhinophores, eyes, and oral tentacles. B) 3D rendering of autofluorescence of the brain in an intact animal embedded in hydrogel. MHD-assisted CLARITY was used to clear the tissue, which was imaged using lightsheet microscopy. The right *rhg* (cyan) and CRG (pink) are shown. Dashed line crosses the *ceg-rhg* connective. C) Z-projection of a fluorescence confocal image for dissected head ganglia with DAPI-labeled nuclei. The CRG and *rhg* ganglia are labeled and colored corresponding to the 3D rendering in 1B. The *bcg* are not shown. Abbreviations: *ceg* - cerebral ganglion, *plg* - pleural ganglion, *pdg* - pedal ganglion, *bcg* - buccal ganglion.

After quality control and cleaning, sequenced raw reads were pseudo-aligned using kallisto (Bray et al. 2016) to a *de novo Berghia* reference transcriptome. The reference transcriptome contained reads from multiple tissues and was enriched for transcripts from head ganglia. The Oyster River Protocol meta-assembly pipeline (MacManes 2018) generated multiple transcriptomes using different assemblers and k-mer values. Orthofinder2 (Emms and Kelly 2018) was used to collapse similar *Berghia* transcripts into phylogenetically determined Hierarchical Orthogroups (HOGs) with predicted proteins from other *de novo* nudibranch transcriptomes, and from genomes of other gastropods such as *Aplysia* and *Lottia*. Annotations for sequences from other gastropods and the output of the EnTAP (Hart et al. 2020) and Trinotate (Bryant et al. 2017) annotation pipelines on the *Berghia* transcriptome were combined

to annotate each HOG. The final reference transcriptome contained 78,000 transcripts representing 48,351 HOGs.

Although each HOG was considered a single annotated “gene”, this overestimates the true number of genes in the genome. However, lacking a genome for *Berghia* at this time*,* we erred on the side of keeping more transcripts to enhance read mapping. Of HOGs, 22,844 contained sequences from *Berghia* and at least one other gastropod, and the remaining 25,507 were *Berghia* only HOGs. Because of the gene-species tree reconciliation performed by Orthofinder2, some *Berghia* sequences were separated from their true orthologs into their own HOG, artificially inflating the number of *Berghia* only HOGs. At least one annotation was appended onto 29,991 HOGs, and the remaining 18,360 HOGs were unannotated.

Single cell transcriptomes

After gene counts for single cells were acquired using bustools (Melsted et al. 2021), data were analyzed using the R package Seurat (Hao et al. 2021). Cells from both the CRG sample and *rhg* sample were combined into a single Seurat object to look for evidence of batch effects. The two samples had similar numbers of cells, unique molecular identifiers (UMIs) per cell, and numbers of genes expressed (Fig. S1), and therefore were combined into a single dataset. After quality control filtering, we recovered transcriptomes for 872 cells from the CRG and 708 cells from the *rhg.* These 1,580 cells segregated into 19 clusters based on similarity of gene expression using FindClusters in Seurat with a resolution of three (Fig 2A, B). Clusters lacking meaningful differences in gene expression (*i.e.*, most genes shared or only log-fold differences in expression of shared genes) were merged based on clustering results from lower resolutions, visualized using Clustree (Zappia and Oshlack 2018) to form single clusters, leaving a final total of 14 clusters.

The cell clusters were annotated using differentially expressed genes to assign putative identities based on the literature, and the sample origin where relevant. There were nine neuronal and five non-neuronal cell clusters found (Fig. 2B, Fig. 3), most of which had cells from both the *rhg* and CRG samples (Fig. 2A). Cluster markers were selected based on differential gene expression between one cluster and all others (Fig 3). In general, in neuronal clusters, the most specific markers were often expressed in fewer than 50% of cells in the cluster, suggesting that these neuronal clusters were still quite heterogeneous. This contrasted with the cluster markers for non-neuronal cell types, where the percentage of cells in the cluster expressing a marker was often much higher (over 90%).

Differential gene expression revealed marker genes for non-neuronal cell type clusters

Molluscan glia do not express canonical glial markers known from other phyla

Three clusters containing putative glial cells share many differentially expressed genes in common compared to other clusters. Glial markers such as glutamine synthetase, support the identity of cells in these clusters as glia (Linser, Trapido-Rosenthal, and Orona 1997) (Fig. 3). We did not find expression of canonical glial markers such as *GFAP* in vertebrates (L. F. Eng 1985; Lawrence F. Eng, Ghirnikar, and Lee 2000) or *repo* in arthropods ((Xiong et al. 1994; Halter et al. 1995) in the *Berghia* reference transcriptome or consequently, in the single cell transcriptomes. This is consistent with recent single cell transcriptomics in the brains of cephalopods molluscs (Styfhals et al. 2022; Songco-Casey et al. 2022; Gavriouchkina et al. 2022). Apolipophorin was used as a glial marker in *Octopus* (Styfhals et al. 2022). A transcript

annotated as an intermediate filament protein, tha same superfamily as GFAP, was differentially expressed in the putative glial clusters (Fig. 3).

Other non-neuronal cells were captured in the brain scRNAseq data

One cluster showed highly differential expression of multiple collagen genes, suggesting that these cells may be fibroblasts or other cells that form connective tissues. The brains of gastropods and other molluscs are surrounded by a cellular sheath, which we did not remove prior to dissection, which may be the source of these cells.

Endothelial and basement membrane components were differentially expressed by putative endothelial cells in the brain. Markers like hepatocyte growth factor receptor and goose-type lysozyme suggest this cluster is composed of endothelial cells potentially lining blood vessels in the nervous system. Hepatocyte growth factor is involved in angiogenesis (Ishizawa et al. 2004; Jung et al. 1994; Sun, Funakoshi, and Nakamura 2002). Goose- (or g-) type lysozymes are part of antimicrobial and immune responses in both invertebrates and vertebrates (Irwin and Gong 2003; Irwin 2014). G-type lysozymes are found in hemolymph (blood) in scallops (González et al. 2022) and are expressed by scallop hematocytes (Shi et al. 2014). Additionally, transgelin, hemicentin, laminin and collagen are all components in basement matrix (BM) in many tissues across animals (Jayadev and Sherwood 2017) and were differentially expressed in the endothelial cell cluster.

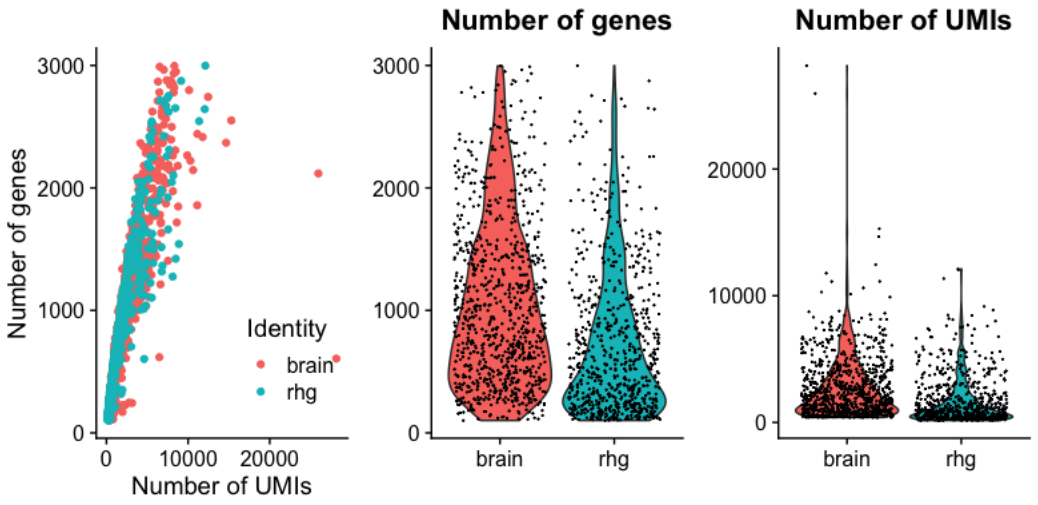

Figure S1: QC plots for both the CRG and rhg samples. The number of cells, genes and UMIs were similar between the two samples.

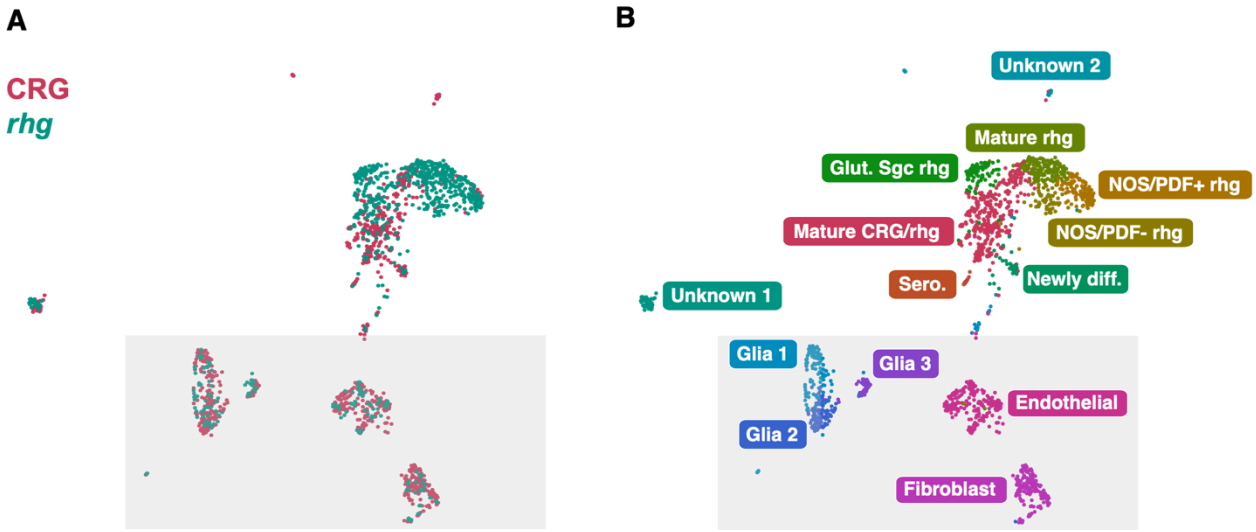

Figure 2: The *Berghia* single cell atlas contains 14 cell clusters, with 9 neuronal clusters and 5 non-neuronal clusters. A) Unifold Manifest Approximation and Projection (UMAP) plot of the *Berghia* single cell RNA-seq dataset from the two samples, the CRG (pink) and *rhg* (cyan). Most clusters are a mix from both samples. B) UMAP plot showing 1580 *Berghia* cells clustered into 14 groups. Non-neuronal clusters are contained within the shaded box.

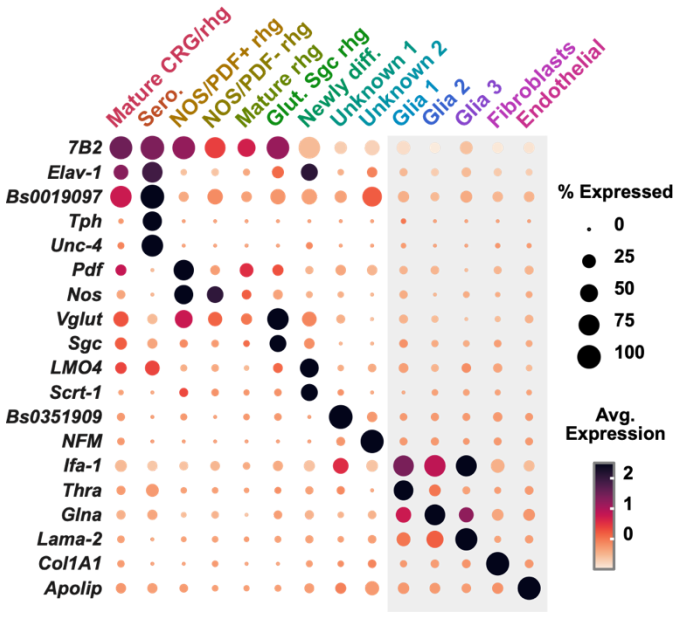

Figure 3: Dotplot of selected marker genes for each cluster. Non-neuronal cell types are boxed in gray. Cluster names and colors correspond to those in Fig. 2B.

Pan-neuronal marker genes label neurons across the *Berghia* brain

The expression of pan-neuronal genes marked candidate neuronal clusters. 865 putative neurons were identified, spread across seven clusters (Fig. 3). Canonical neuronal markers like *elav* (Fig. 3, Fig. 4A) were expressed primarily in four clusters. Oddly, *elav* was not well represented in clusters primarily containing *rhg* neurons, where expression was mostly absent or sparse (Fig. 4A). Despite the low number of neurons with mRNA for *elav-1* in the single cell dataset, an HCR probe for *elav-1* mRNA labeled most neurons, including neurons in the *rhg* (Fig. 4D), as expected from *elav* expression in neurons in other animals.

Another pan-neuronal marker was neuroendocrine protein *7B2*. This gene is expressed in most neurons in other animals, including molluscs(Marcinkiewicz, Touraine, and Chrétien 1994;

Spijker et al. 1999; Hwang et al. 2000). *7B2* showed high mRNA abundance and distribution of *7B2* mRNA in all putative neuronal clusters regardless of sample origin (see Figs. 3 & 4C). Low, sparse mRNA abundance for *7B2* was also found in a cluster of putative non-neuronal glial and endothelial cells, consistent with previous findings in mouse(Seidel et al. 1998). *7B2,* is the molecular chaperone for *prohormone/neuroendocrine convertase 2* (*pc2*), and *pc2* mRNA, was also highly abundant in neuronal clusters. The expression of *7B2* and its molecular partner support the hypothesis that the cells in these clusters are neurons.

Finally, we found mRNA for an unannotated gene, *Bs19097,* present primarily in neuronal clusters and expressed ubiquitously in neurons across all ganglia (Fig. 3 & 4B). When labeled using multiplexed HCR, there was extensive co-expression of *elav-1* (Fig 4D)*, Bs19097* (Fig. 4E, F)*,* and *7B2* (Fig. 4G), in addition to overlapping expression in presumptive neuronal clusters in the single cell dataset (Fig. 4A-C). Because the expression patterns for *Bs19097* closely match known pan-neuronal markers, we are confident in its identity as a pan-neuronal marker, despite its anonymity as a gene.

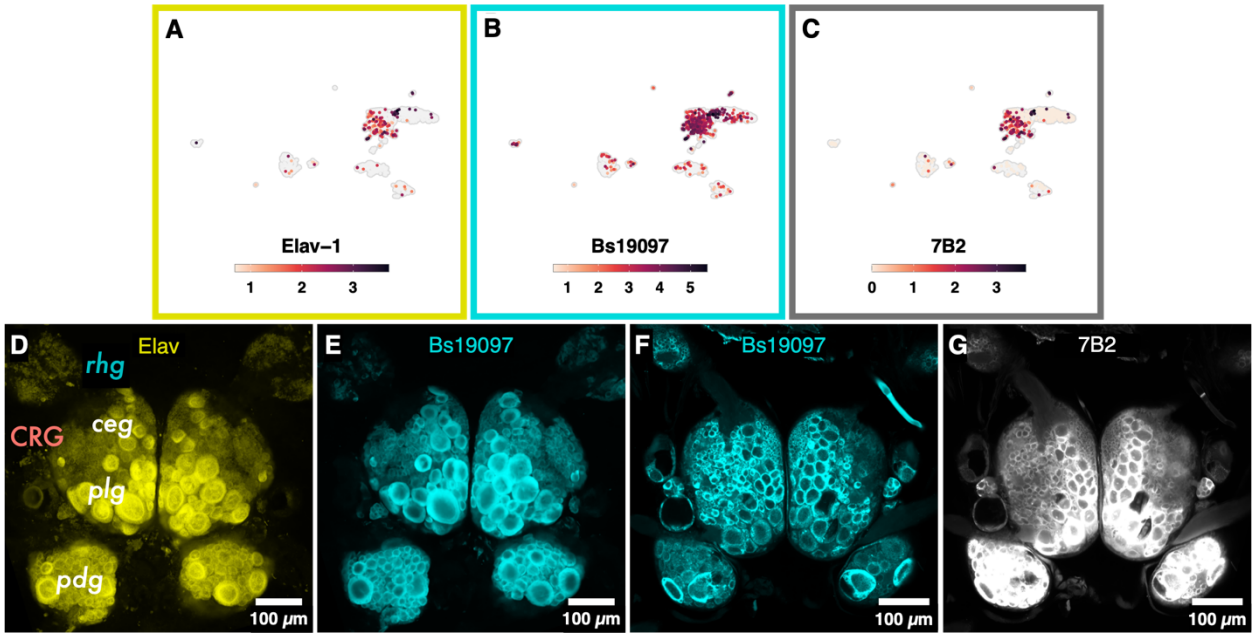

Figure 4: Putative pan-neuronal marker genes identify neuronal clusters. A-C) UMAP plots showing mRNA abundance and distribution of A) *elav*, B) unannotated transcript *Bs19097,* and C) *7B2*. D-G) Single optical sections of a fluorescence confocal z-stack using HCR to label mRNA for pan-neuronal markers: *Elav-1* (D)*,* unannotated transcript *Bs19097* (E,F), *7B2,* the molecular chaperone protein for *prohormone/neuroendocrine convertase 2* (G)*.* D and E are the same sample. F and G are the same sample.

The expression patterns of both candidate genes and cluster markers subdivide neuronal classes across the entire CNS.

Candidate genes that subdivide neurons into large classes or groups were examined. These included markers for differentiating neurons, neurotransmitters, neuropeptides, and transcription factors. Most often, these markers spanned multiple neuronal clusters and by themselves did not distinguish clusters. Primary exceptions for this pattern were markers for newly differentiated neurons, which together cleanly delineated this cluster in the atlas. The serotonergic neurons also had highly specific cluster markers in the atlas. Overall, regardless of the specificity of a gene to a cluster in the single cell atlas, visualizing the expression in the brain revealed

neuronal classes, with a wide diversity of neurons of different sizes, numbers, and locations within and between ganglia.

Newly differentiated neurons

Genes like *LMO4, Sox6*, *Sox2*, *Scratch1*, and are associated with neuronal differentiation. Only one cluster in the scRNAseq atlas expressed this whole suite of genes, suggesting that the cells in this cluster were newly differentiated neurons (Fig. 5). *LMO4* is a cofactor with *neurogenin* for neural differentiation (Asprer et al. 2011). *Sox6* and *Sox2* work together to inhibit neural differentiation in vertebrates (Lee et al. 2014; Li et al. 2022), with *SoxB1* (homolog of vertebrate *Sox* family genes) key to neuroblast formation in *Drosophila* (Buescher, Hing, and Chia 2002). *Scratch1* is important for neural differentiation in *C. elegans*, mammalian cell culture, and *Drosophila* (Nakakura et al. 2001; Manzanares, Locascio, and Nieto 2001; Nieto 2002). In mammalian forebrain, *Scratch* genes act downstream of proneural genes like *neurogenin* and *Ascl1* and control the initiation of migration of newly differentiated neurons (Itoh et al. 2013).

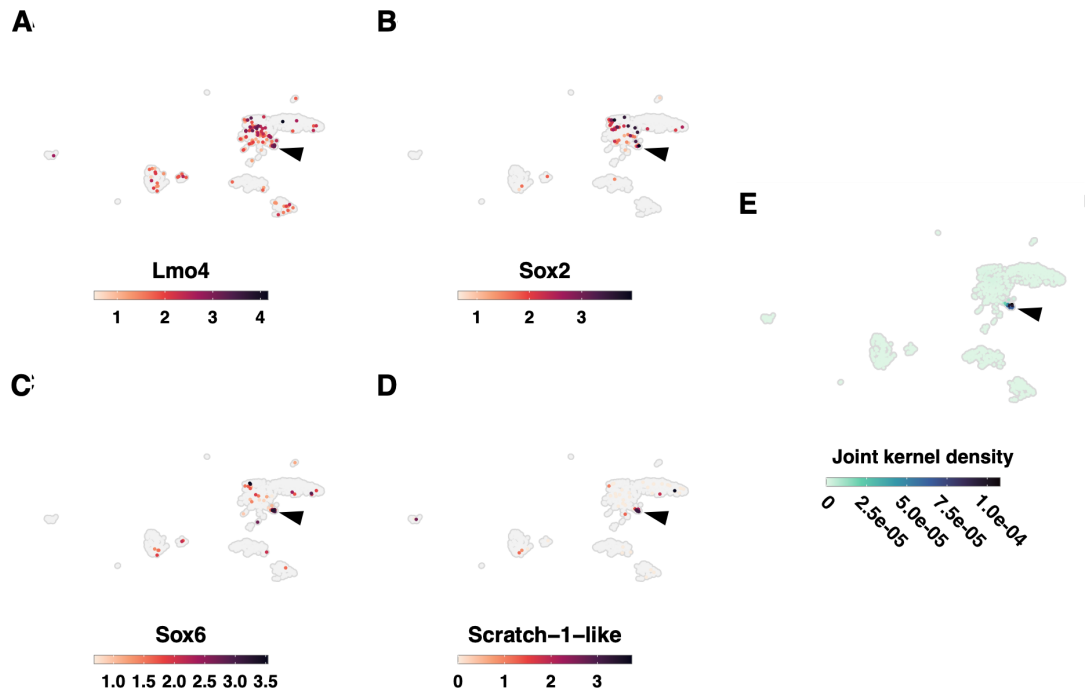

Figure 5: Marker genes expressed in a cluster containing newly differentiated neurons. A) *Lmo4*, B) *Sox2,* C) *Sox6,* D) *Scratch-1.* E) Joint kernel density plot showing the peak of overlapping expression of the four genes specifically in the newly differentiated neuron cluster (arrowheads).

Major small molecule neurotransmitters: acetylcholine, glutamate, and serotonin

We looked for the expression of candidate enzymes and transporters associated with small molecule neurotransmitters. In the single cell atlas, mRNAs were found for *Vesicular glutamate transporter* (*Vglut*, glutamate), *Choline acetyltransferase* (*Chat,* acetylcholine*)*, *Glutamate decarboxylase* (*Gad*, GABA), *Tryptophan hydroxylase* (*Tph*, serotonin), *Histidine decarboxylase* (*Hd*, histamine), and *tyramine beta-hydroxylase* (*Tbh*, octopamine). There was no evidence of mRNA for *tyrosine hydroxylase*, the rate-limiting enzyme for catecholamine synthesis, but this may be the result of low gene expression, the small number of neurons captured, and the rarity

of catecholaminergic neurons in the CRG of gastropods (Croll 2001) rather than true absence. A total of 467 neurons (~50%) possessed mRNAs for at least one of these genes. Using HCR, we visualized mRNAs for the most prevalent neurotransmitter-associated genes: *Vglut*, *Chat*, and *Tph* (see Fig 6D-I). A large percentage of the neurons in the head ganglia expressed *Vglut*, *Chat*, or *Tph.* There was co-expression of at least two neurotransmitters in a small number of neurons for *Vglut, Chat,* and *Tph* (Fig. 6H,I).

Glutamate appears to be the most prevalent neurotransmitter in the head ganglia. *Vesicular glutamate transporter* (*Vglut)* loads glutamate into vesicles to be released at synapses. One *Vglut* transcript was expressed in 327 neurons from both the CRG and *rhg* scRNAseq samples (Fig 6A). The spatial distribution of *Vglut* mRNA in the brain supports the single cell data– HCR for *Vglut* mRNA labeled many neurons and at relatively high levels as a transporter (Fig 6D). *Vglut* HCR also labeled just one of the photoreceptors in the eye (Fig 6D, arrowhead). In the nudibranch *Hermissenda*, both acetycholine and GABA have been suggested as neurotransnmitters in eye photoreceptors (Heldman et al. 1979; Schultz and Clark 1997).

Acetylcholine was also widespread in neurons throughout the head ganglia. *Choline acetyltransferase* (*Chat*), the rate-limiting enzyme for acetylcholine synthesis, was expressed in multiple clusters of mature neurons from the CRG and *rhg* scRNAseq dataset (Fig 6B). There were 108 neurons containing *Chat* mRNA in the single cell atlas. When viewed with *in situ* HCR, *Chat* was present in many neurons (Fig 6E), but fewer than expressed *Vglut* (Fig 6D, H). This is consistent with the percentage found in the brain of the slug *Limax* (D'Este et al. 2011).

Serotonin was not as widespread as the other two neurotransmitters. mRNA for *tryptophan hydroxylase (Tph)*, the rate limiting enzyme for serotonin synthesis, was found exclusively in a cluster containing only 8 neurons in the single cell atlas (Fig 6C). *Tph* mRNA visualized using

HCR in the brain was more prevalent than suggested from the single cell data (Fig 6F), indicating a sampling bias in the scRNAseq data likely due to the large (>40 um) soma sizes of these neurons that excluded them from the microfluidics chip. Unlike *Vglut* and *Chat,* HCR for *Tph* was much more spatially restricted. The majority of *Tph* expressing cells were found in the pedal ganglia, and a much smaller number (< 20) were found in the cerebral-pleural ganglia (Fig 6F). A small number of pedal ganglion neurons appear to express both *Tph* and *Chat* (Fig. 6I) Although a couple of *rhg* cells possess *Tph* mRNA in the single cell atlas, we found no evidence of *Tph* expression in the *rhg* using HCR (Fig 6C). The distribution of *Tph* neurons in the *Berghia* brain matches the highly conserved pattern of serotonin IHC seen in other nudibranch species (Newcomb, Fickbohm, and Katz 2006).

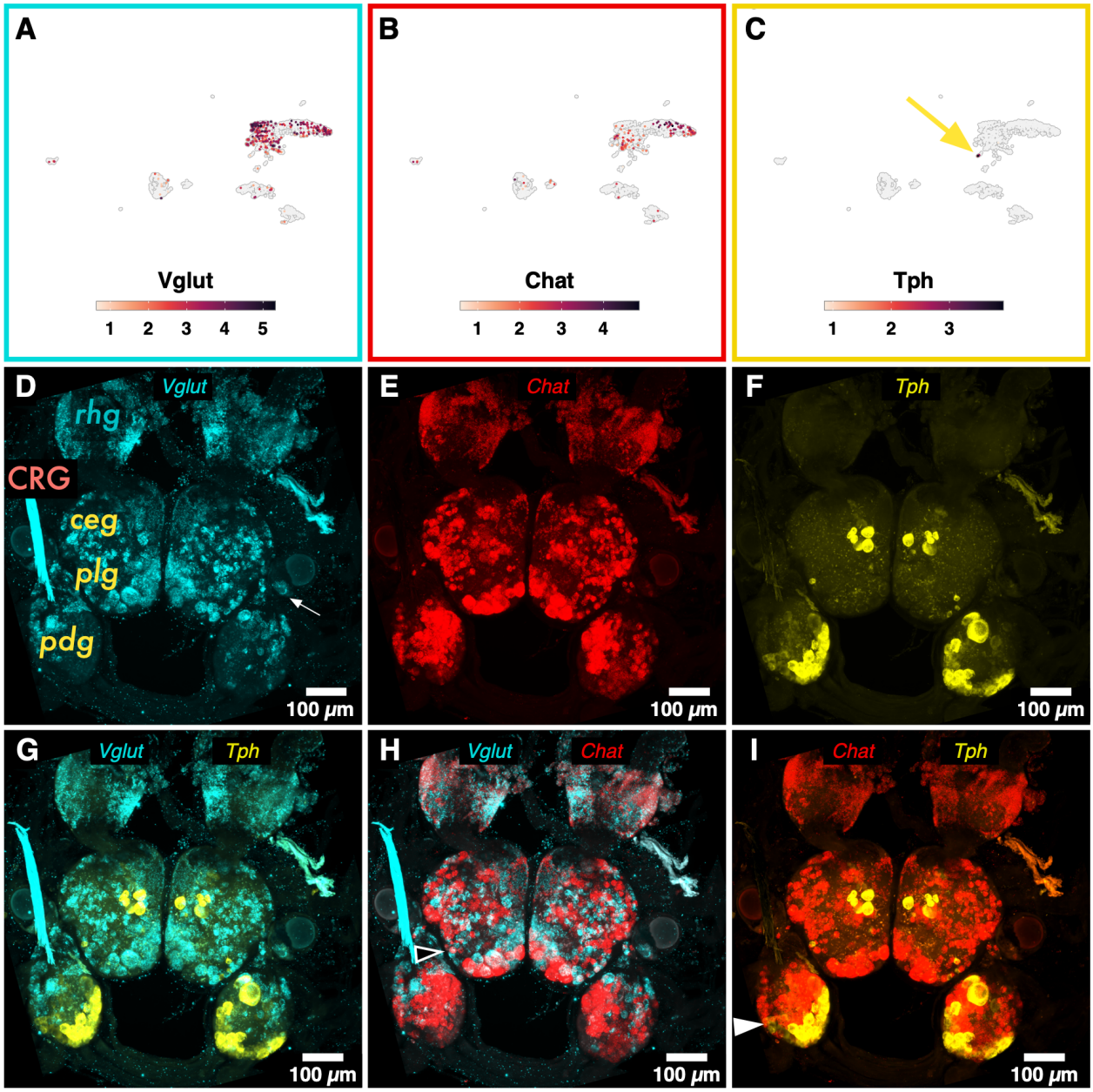
A
Vglut
1 2 3 4 5
B
Chat
1 2 3 4
C
Tph
1 2 3
D
Vglut
rhg
CRG
ceg
plg
pdg
100 µm
E
Chat
100 µm
F
Tph
100 µm
G
Vglut
Tph
100 µm
H
Vglut
Chat
100 µm
I
Chat
Tph
100 µm

Figure 6: Abundance and visualization of mRNA for neurotransmitter-associated enzymes and transporters in *Berghia*. A-C) UMAP plots showing mRNA abundances of *Vglut* (A)*, Chat* (B), and *Tph* (C) *across* neuronal clusters. The yellow arrow points to the small cluster of *Tph*+ neurons. D-F) Z-projections of a fluorescence confocal image using HCR to label *Vglut* (D)*, Chat* (E)*,* and *Tph* (F)*.* The white arrow in panel D points to a *Vglut*+ photoreceptor in the eye. G-H) Pairwise double labeling of *Vglut* and *Tph* (G), *Vglut* and *Chat* (H), and *Chat* and *Trph* (I). The open white arrowhead in H) points to a neuron double-labeled for *Vglut* and *Chat*. The solid white arrowhead in I) points to a neuron double-labeled for *Chat* and *Tph*. However, most of the neurons are labeled for only one of the genes. All images D-I are in the same sample.

Transcription factors define brain regions and neuronal classes in expression patterns like those seen in other bilaterians.

Six3/6 is involved in many different developmental processes in animals, including anterior brain and eye development (Bernier et al. 2000; Seimiya and Gehring 2000). While *Six3/6* mRNA was found in neurons in multiple clusters in the atlas, it is highly differentially expressed in the glutamatergic *Sgc rhg* neuron cluster (Fig 7A). Using HCR to visualize *Six3/6* mRNA*,* expression in the CRG was completely restricted to *ceg* neurons and was distributed among many *rhg* neurons (Fig 7B). These are the most anterior ganglia of the major head ganglia (see Fig. 1B). Anterior expression is consistent with *Six6* expression in developing vertebrate brains (Oliver et al. 1995). *Six3/6* also has a role in eye development in multiple animal phyla (Seo et al. 1998; Seimiya and Gehring 2000), but using HCR, there was no expression of *Six3/6* in the eye. However, a single neuron within the optic ganglia was labeled for *Six3/6. Optix* (the *Six3/6* homolog in *Drosophila)* regulates and demarcates the larval optic lobe (Gold and Brand 2014).

Delta is another broadly expressed transcription factor in the single cell data, although there was a higher density of *Delta* expressing neurons in the *rhg,* and *Delta* was differentially expressed by *rhg* neurons (Fig. 7C). Both *Six3/6* and *Delta* were differentially expressed in the glutamatergic *Sgc rhg* neuron cluster in the scRNAseq atlas (Fig. 7A,C). Many neurons in the

rhg expressed both *Six3/6* and *Delta* (Fig. 7G). *Delta* is part of the *Wnt* pathway typically associated with early development of major aspects of nervous systems across animals (Bettenhausen et al. 1995; Henrique et al. 1995; Chitnis et al. 1995; Kawaguchi et al. 2008). *Delta* was found in the cluster of newly differentiated neurons of the single cell atlas, consistent with its role in development. However, *Delta* mRNA was found in neurons across all head ganglia in presumably mature neurons in adult brains (Fig 7D). Despite its canonical role in early development, expression of *Delta* in mature neurons in adults has also been described in *Drosophila* and vertebrates (Cornbrooks et al. 2007; Stump et al. 2002). In *C. elegans*, *Delta* (*lin-12*) expression also influences locomotor behavior without changing cell type identities, suggesting a role for *Delta* (Chao et al. 2005). Many of the *Delta* expressing neurons differ in size and location, suggesting that *Delta* may be part of the gene expression profiles of multiple neuron types in *Berghia*'s brain (Fig 7D).

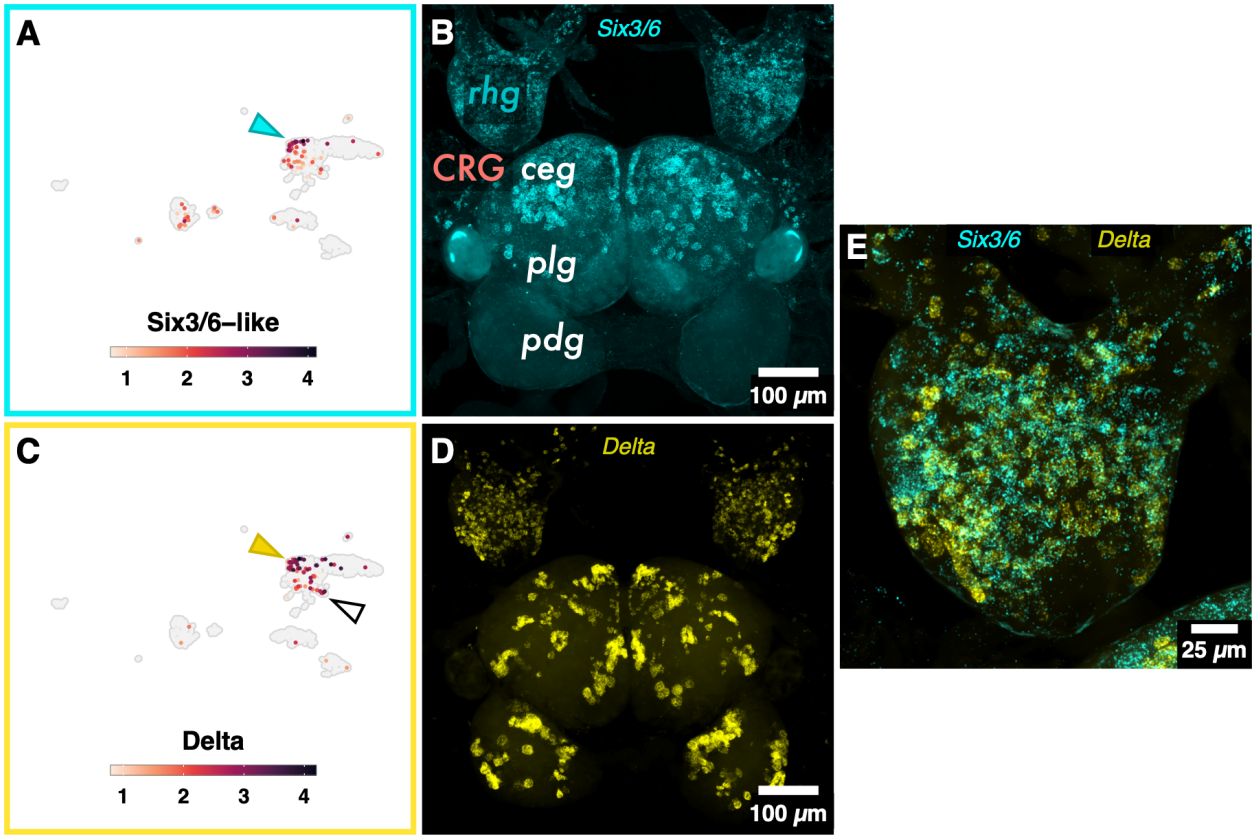

Figure 7: Transcription factor expression can help define different brain regions**.** A) *Six6* mRNA was most abundant in *Sgc rhg* neurons in the single cell atlas and was differentially expressed in this cluster. B) Z-projection of a fluorescence confocal image using HCR to label *Six6* mRNA. It was almost exclusively present in neurons in the anterior-most ganglia, the rhinophore ganglia and the cerebral ganglia. C) *Delta* mRNA is concentrated in the *Sgc rhg* (yellow arrowhead) and differentiating neuron (black arrowhead) clusters in the single cell atlas. *Delta* was differentially expressed in the *Sgc rhg* neuron cluster. D) Z-projection of a fluorescence confocal image using HCR to label *Delta* mRNA showed it widely distributed across the ganglia. Many neurons in the *rhg* contain *Delta* mRNA, some of which likely correspond with the *Sgc rhg* neurons. E) Higher magnification of the *rhg* showing co-expression of *Six3/6* and *Delta* in many of the same neurons. B,D, E are the same sample.

The neuropeptide complement found in the *Berghia* CNS includes broadly conserved, bilaterian genes as well as others that are lineage specific.

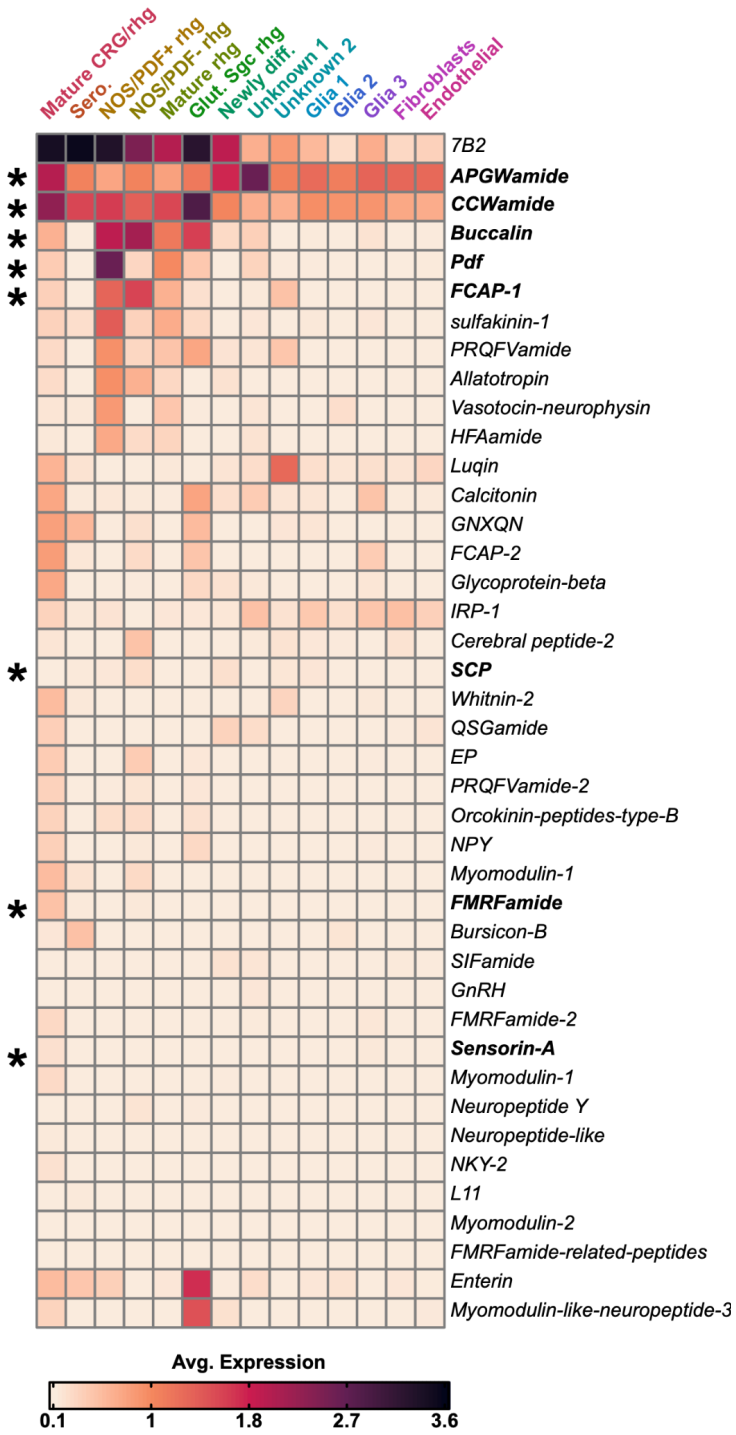

Fig 8: Over 40 types of neuropeptides were found within the atlas, and their expression varied by cluster. The mature CRG/*rhg* neuron cluster contained the largest number of neurons, and showed the largest and most varied expression of neuropeptides between the clusters. Only a few neuropeptides were restricted to specific clusters. *Luqin* was primarily expressed in Unknown 1 neurons. *Enterin* and *myomodulin* expression marked neurons in the glutamatergic, *Sgc+ rhg* cluster. Asterisks indicate neuropeptides that were selected for visualization using HCR in Fig. 9.

We found expression of at least 40 out of a minimum set of 65 molluscan neuropeptides(De Oliveira, Calcino, and Wanninger 2019) in the single cell transcriptomes (Fig. 8). The large cluster of mature CRG/*rhg* neurons showed high average expression of most neuropeptides in a small number of neurons, consistent with our hypothesis that this cluster consists of many rare neuron types. *APGWamide* (*APGW* or *cerebral peptide*) was one of the most highly expressed genes overall, and mRNA found in many different neuronal and non-neuronal cells. Visualization of *APGW* mRNA in the CRG and *rhg* reflected both the wide range of cells expressing this neuropeptide, most of which also showed extremely high levels of expression (Fig. 9A). There was sufficient *APGW* mRNA in individual neurons that extended out of the somata into their axons to identify projection patterns. Another interesting example was *CCWamide,* which was differentially expressed in the largest neuronal clusters (Fig. 9B). *CCWamide* was recently identified in a broad search for neuropeptides in annelids, molluscs, and other lophotrochozoan phyla (Williams et al. 2017; Thiel et al. 2021). Its expression pattern in molluscan brains was not unknown. *CCWamide* mRNA was found in a significant portion of cells in our single-cell atlas, in both neurons and non-neuronal cell types. (Fig 8). Visualizing *CCWamide* with HCR reflected the high abundance and broad expression of *CCWamide* seen in the single cell atlas (Fig 9B).

Other neuropeptides showed more restricted expression. Except for some neurons in the mature CRG/*rhg* cluster, *luqin* is found only in the cluster of unknown 2 neurons, and *IRP-1* is found in the Glial 3 cluster. *Pigment dispersing peptide* (*Pdf*, also called *Cerebrin*, Fig. 9C) and

one transcript of *Feeding circuit-activating peptide* (*Fcap*, Fig. 9E) were differentially expressed in *Nos/Pdf+ rhg* cluster. *Buccalin*, a putative homolog for allatostatin-A (Veenstra 2010), was also differentially expressed in this cluster (Fig. 9D). Despite differential expression in the *Nos/Pdf+ rhg* neuron cluster, mRNA for these peptides was found in other neuronal clusters, and spatially distributed in the CNS in many, if not all, ganglia. For example, HCR shows *Pdf* mRNA is also highly expressed by a few distinct CRG neuron types in the *ceg* (Fig. 9C). Besides its expression in small *rhg* neurons, *Fcap* is also expressed in some of the largest neurons within the lateral region of the *rhg,* as well as many of the large neurons of the *ceg* and *plg* (Fig 9E). One large and 4-5 other smaller *bcg* neurons also express *Fcap* (Fig. 9E). Numerous *buccalin*-expressing cells were found primarily in the *rhg*, *ceg,* and *pdg*, but only a handful were present in the *plg* (Fig. 9D).

In addition to investigating neuropeptides that were differentially expressed in the single cell atlas, we also looked for expression of neuropeptide candidates gleaned from the literature, including *Small cardioactive peptide* (*SCP*) (Fig. 9F) and *FMRFamide* (Fig. 9G). Like differentially expressed neuropeptides, these candidate neuropeptides were present in neurons of many different positions and size classes within the CRG and *rhg*.

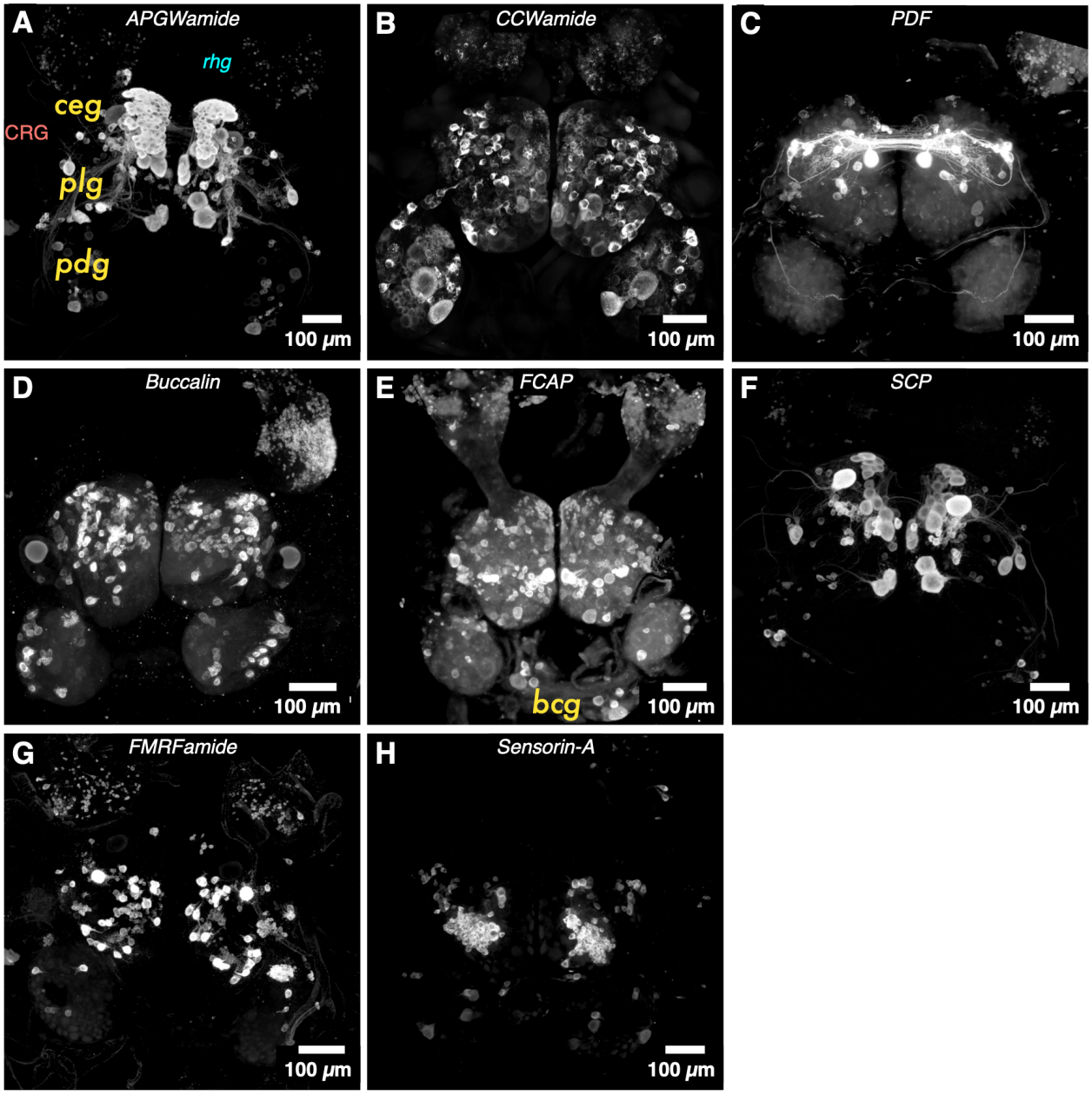

Figure 9: Neuropeptide expression was distinct for each gene, and varied greatly in the number of neurons and their distributions across the ganglia. Z-projections of a fluorescence confocal image using HCR to label mRNA for eight neuropeptides: APGWamide (A), CCWamide (B), PDF (C), Buccalin (D), FCAP (E), SCP (F), FMRFamide (G), and Sensorin-A (H).

Many *rhg* neurons are distinguished by genes involved in nitric oxide (NO) signaling.

NOS-expressing rhg neurons

Two clusters of *rhg* neurons shared expression of *Chat* and *Nitric oxide synthase* (*Nos),* but were distinct in whether they contain mRNA for *pigment dispersing factor* (*Pdf)* (Fig. 10A,B). Using HCR to label mRNA for *Nos* and *Pdf,* two populations of neurons were found that likely corresponded to the *Nos*/*Pdf*+ and *Nos*/*Pdf*+ cells in the single cell dataset. (Fig. 10D-F). Both *Pdf* and *Nos* mRNA were also present in a small number of CRG neurons in the single cell atlas and when visualized in the brain (Fig. 10C).

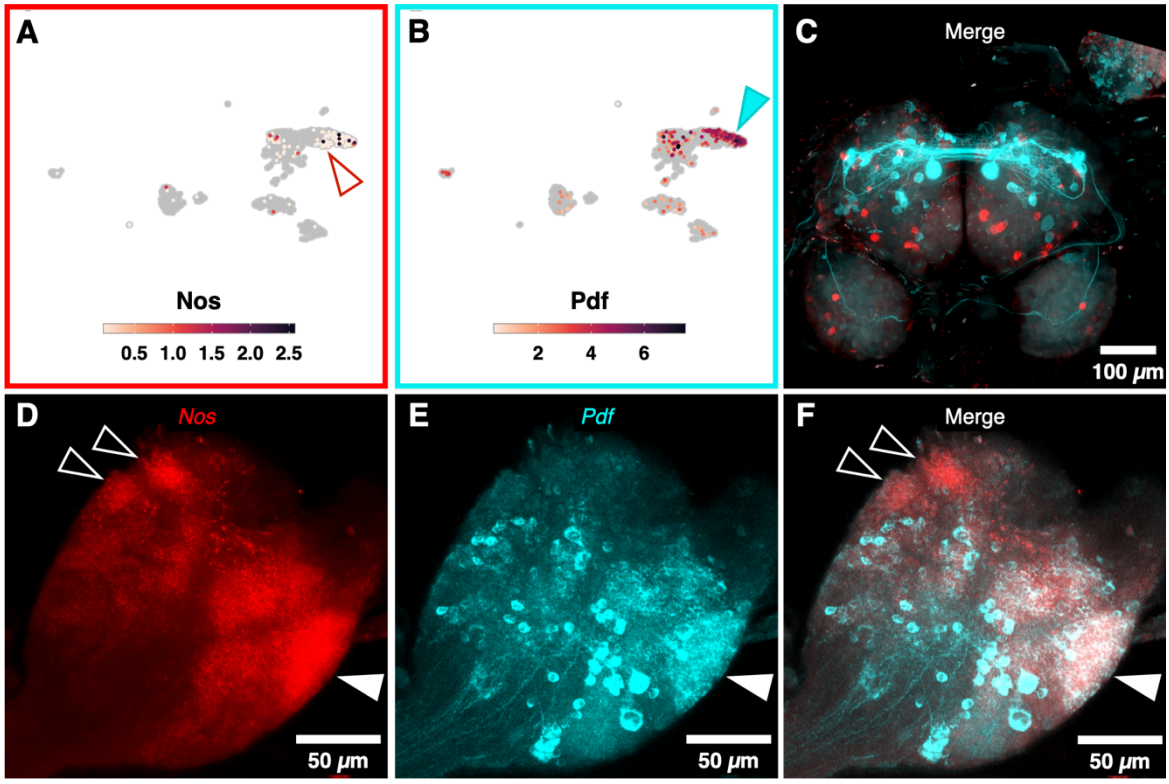

Figure 10: Nos+/Pdf+ and Nos+/Pdf- are separate populations of cells within both the CRG and *rhg.* UMAP plots of the expression of A) *Nos* and B) the neuropeptide *Pdf* in the single cell atlas. C) Z-projection of a fluorescence confocal image using HCR to label mRNA in for *Nos* (red) and *Pdf* (cyan) in the CRG. A pair of medium sized *Pdf*+ neurons sit near the midline in the *ceg* and send projections contralaterally. The projections appear to meet other *Pdf*+ neurons in the *ceg,* which together form a distinct loop throughout the ganglia. *Nos*+ neurons were typically smaller and distributed mostly as single cells across all the ganglia. D-F) Z-projection of a fluorescence confocal image using HCR to label mRNA in the rhinophore ganglion for: *Nos* (D)*, Pdf* (E)*,* and the merge of the labels (F). Open arrowheads point to populations of cells that express *Nos* but not *Pdf*. The closed arrowhead shows a population of cells that co-express these genes.

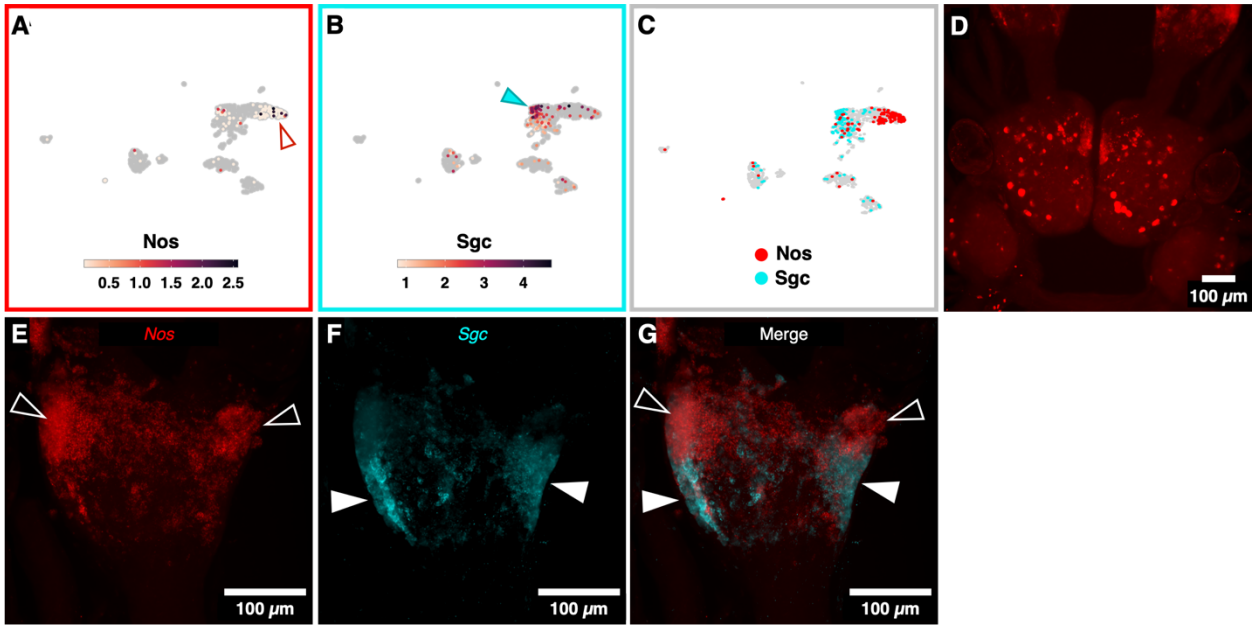

Figure 11: Neurons expressing either *Nos* and *Sgc* were separated into different clusters in the single cell atlas that was reflected in their expression within the *rhg*. UMAP plot showing expression of *Nos* (A)*, Sgc* (B)*,* and mutually exclusive expression of the two genes mapped onto the clusters (C). D) Z-projection of a fluorescence confocal image using HCR to label mRNA for *Nos* in the CRG. *Nos* expressing neurons were in the *rhg* and the CRG. E-G) Z-projection of a fluorescence confocal image using HCR to label mRNA in the rhinophore ganglia for *Nos* (D)*, Sgc* (E)*,* and the merged image (F). There were distinct populations of cells expressing each gene in the *rhg.*

The other primarily *rhg* neuron cluster in the scRNAseq atlas was marked by the expression of *Vglut* and *soluble guanylate cyclase* (*Sgc*). *Sgc* is the receptor for nitric oxide (NO) (Martin et al. 2005), raising the possibility that these neurons may receive NO as signals, potentially from

other *rhg* neurons that express *Nos.* When co-labeled with *Nos* in the *rhg*, mRNA for the two genes were mostly mutually exclusive (Fig. 11). There appeared to be fewer, larger *rhg* neurons that express *Sgc*, which were interspersed among *Nos* expressing neurons (Fig 11G).

Specific neuronal cell classes and types are distinguishable based on their molecular signatures.

Some *Berghia* neurons express the bilaterian molecular signature of mechanosensory neurons.

Peripheral sensory neurons, particularly mechanosensors, and interneurons that synapse with mechanosensory neurons express *Brn3*, *Drgx*, *Islet-1*, *Vesicular glutamate transporter* (*Vglut*), and *Lhx3/4* across bilaterian phyla, including molluscs(Nomaksteinsky et al. 2013). *Brn3* and *Vglut* mRNAs localized to neurons in the *plg*, consistent with the known mechano- and nociceptive circuits in *Aplysia* (Walters, Bodnarova, and Billy 2004). The neuropeptide *Sensorin-A* (*SenA)* was expressed along with *Brn3*+ mechanosensory neurons in *Lymnaea,* including homologs of s-cells in other nudibranchs (Nomaksteinsky et al. 2013). However, most *Brn3*+ neurons in the atlas were not S*enA*+. A small number of neurons within the larger mature CRG/*rhg* atlas cluster were both *SenA*+ and *Brn3*+ (Fig. 12). Consistent with co-expression results from the atlas, HCR for these genes showed co-expression in only a few neurons (Fig. 12, arrowheads). The s-cell homologs in *Berghia* consisted of 15+ small *SenA*+ neurons. These cells did not also express *Brn3*, but there were 1-2 somewhat larger Brn3+ neurons nestled among them. *Berghia* S-cell were glutamatergic, based on their expression of *Vglut,* seen both in the atlas and using HCR. S-cells in other nudibranchs are also glutamatergic (Megalou, Brandon, and Frost 2009).

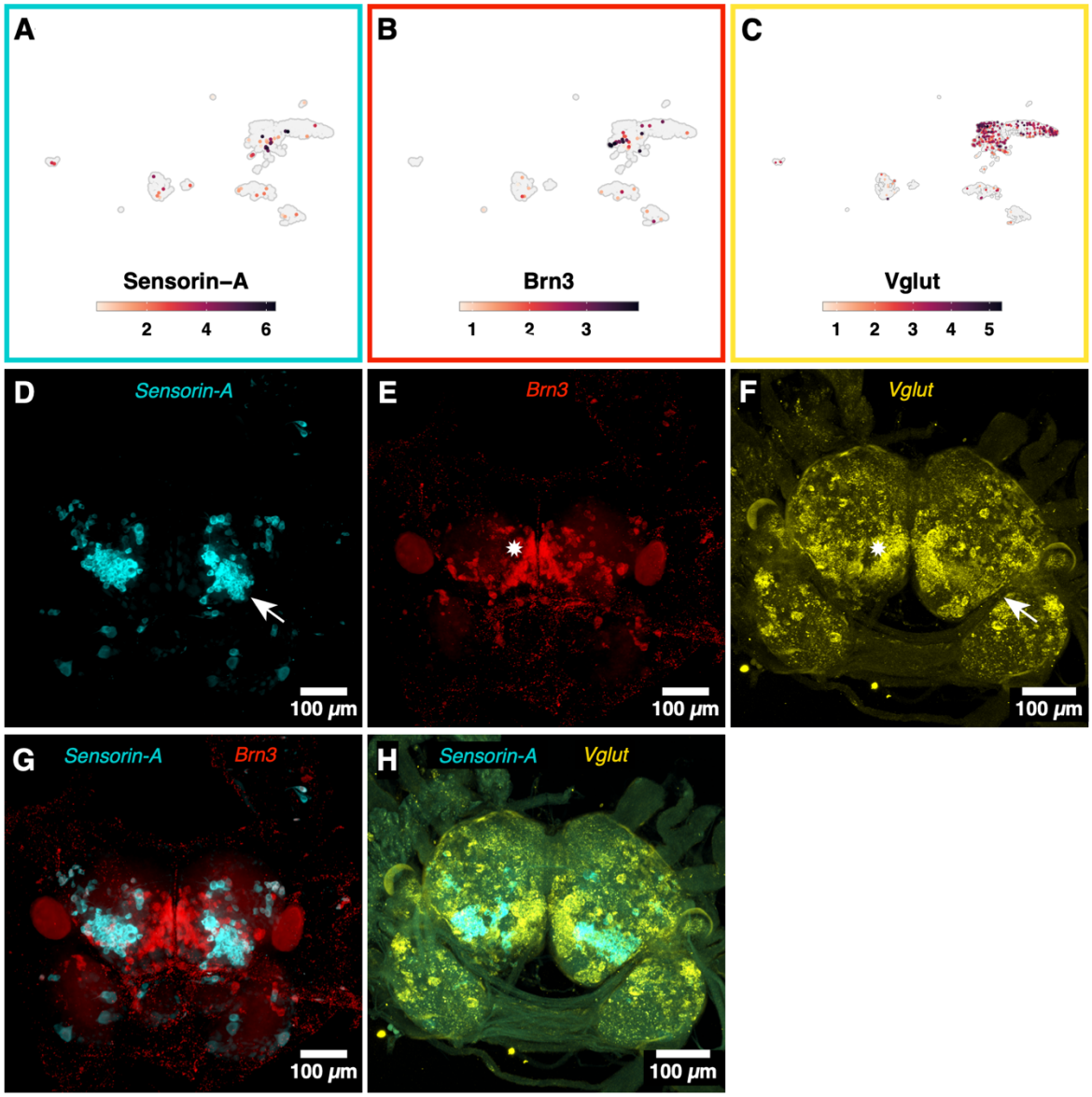

Figure 12: Co-expression of *Vglut* in *Brn3*+ cells indicates mechanosensory neuronal identity. A-C) UMAP plots showing expression of *Sensorin-A*, *Brn3* and *Vglut* in the single cell dataset. Z-projection of a fluorescence confocal image using multiplexed HCR to label mRNA for D) *Sensorin-A*, and E) *Brn3* in the same sample. F) Z-projection of a fluorescence confocal image HCR to label mRNA for *Vglut.* White arrow indicates the likely homologs of the "s-cells" known from other nudibranchs, expressing both *Sensorin-A* and *Vglut*. G) A merged z-projection of fluorescence confocal images of multiplexed HCR for *Sensorin*-A and *Brn3* in the same sample. H) A merged z-projection of fluorescence confocal images of multiplexed HCR for *Sensorin-A* and *Vglut* in the same sample.

Transcription factor Unc-4 is associated with serotonergic efferent neurons in *Berghia,* rather than cholinergic motor neurons as seen in *C. elegans* and *Drosophila.*

Unc-4 underlies specification of motor neurons in both *C. elegans* and *Drosophila* (Pflugrad et al. 1997; Lacin et al. 2020). Motor neurons in these species are also cholinergic and express *Chat*, and *Unc-4* is known in *Drosophila* to repress a GABAergic cell fate leading to a cholinergic one ((Lacin et al. 2020). Surprisingly, in the atlas, *Unc-4* and *Solute carrier family 46 member 3* (*Scf46m3*) were differentially expressed along with *Tryptophan hydroxylase* (*Tph*). Here, *Tph* mRNA was restricted to a small cluster (8 cells), while *Unc-4* and *Scf46m3* mRNAs were found more widely (Fig. 13). Consistent with the co-expression seen in the single cell data, *Unc-4* and *Scf46m3* were co-expressed in CRG neurons along with *Tph*, though both genes were also expressed in a small number of neurons that did not express *Tph* (Fig. 13). As the rate-limiting step in serotonin production, *Tph* was expected to be found only in serotonergic neurons. Further supporting the specificity of *Unc-4* and *Scf46m3* to serotonergic, rather than cholinergic, neurons was the lack of overlapping *Chat* and *Tph* mRNA in the atlas. Visualizing mRNAs for *Chat* and *Tph* with HCR showed overlap in only a small handful of neurons (see Fig. 6I).

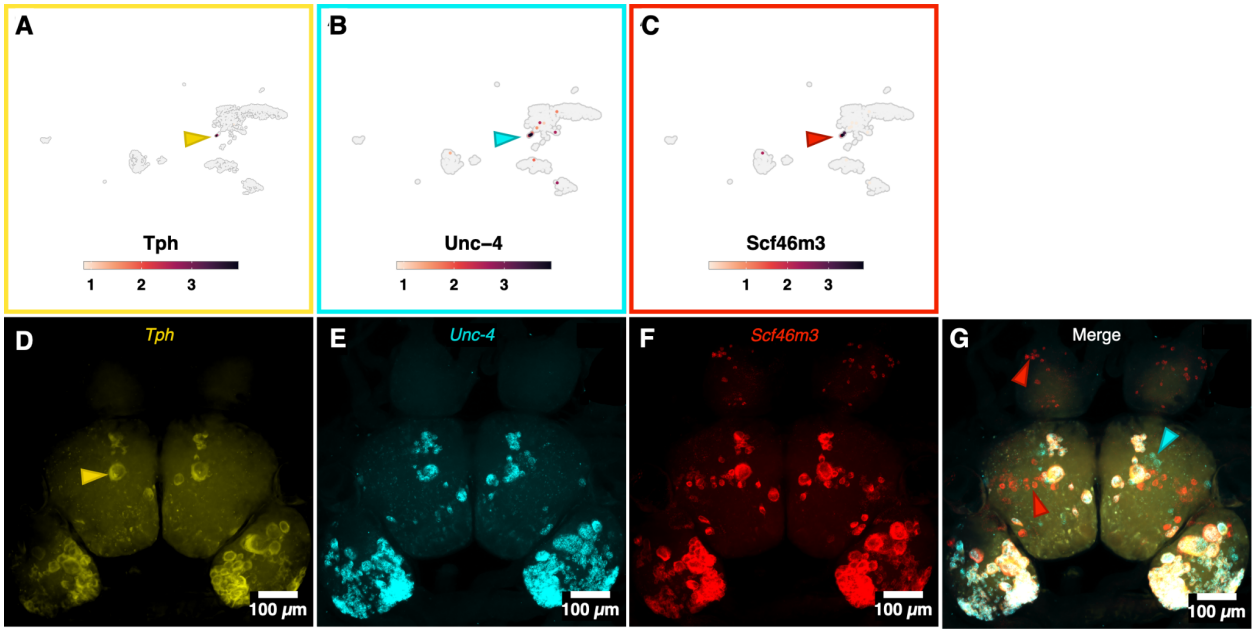

Fig 13: HCR labeling shows mRNA for *Tryptophan hydroxylase*, *Unc-4* and *Solute carrier family 46 member 3* (*Scf46m3*) were co-expressed in serotonergic neurons. A-C) UMAP plots showing mRNA abundances for A) *Tph*, B) *Unc-4*, and C) *Scf46m3*. Arrowheads point to the cluster where all three genes are found. D-G) Z-projection of a fluorescence confocal image using HCR to label D) *Tph*, E) *Unc-4,* and C) *Scf46m3.* The yellow arrowhead in D) points to the likely homolog of the *Aplysia* metacerebral cell in *Berghia*. G) The merged image showing the overlap of these 3 genes. Red arrowheads point to examples of neurons expressing only *Unc-4*. The cyan arrowhead points to an example of neurons expressing only *Scf46m3*.

Unbiased, *de-novo* detection of molecular signatures for identifiable neuron types

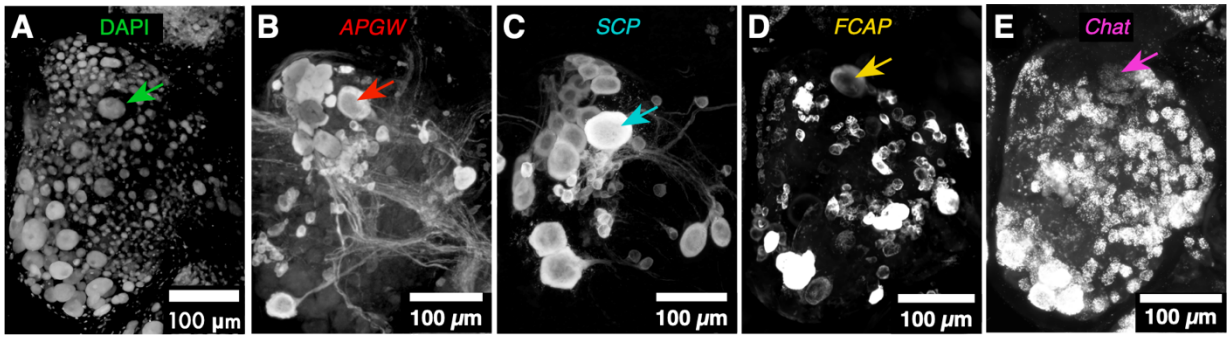

Figure 14: Molecular fingerprint for the giant ventral peptidergic neuron was assembled by analyzing different images of gene expression patterns with Z-projection of a fluorescence confocal image using HCR. Each image shows half of the *Berghia* CNS, and arrows indicate the same identifiable neuron in each, for A) nuclei labeled with DAPI, B) *APGWamide*, C) *SCP*, D) *FCAP* and E) *Chat.* The cell identity is consistent across individual *Berghia* CRG samples. All panels are from different samples.

One identifiable neuron type is a giant, bilaterally symmetrical neuron, which sits on the ventral surface of the *ceg,* near the anterior most region of the ganglion. It is surrounded by a field of much smaller, equally sized neurons and is the largest of neurons in the ventral *ceg* (Fig. 14A). Due to its unique size and location alone, it was straightforward to identify this neuron in images of the ventral surface of the CRG using a nuclear label. This neuron was seen in images for pan-neuronal genes, as expected, but also multiple neuropeptides, including *APGWamide, SCP,* and *FCAP.* Besides neuropeptides, the neuron was observed in HCR images for the enzyme *Chat.*

Unannotated genes are key to differentiating neuron clusters/groups/types.

One striking feature of the top markers for all clusters was the abundance of unannotated genes that were differentially expressed (Fig. 15). Unannotated HOGs represented 38% of the total number of HOGs. The high percentage of unannotated HOGs highlights the historical lack of molecular and functional data to characterize these clade-specific genes found in gastropods and other molluscs. Of unannotated HOGs, only 13% (2,448) were shared among *Berghia* and at least one other gastropod, and the remaining 87% (15912) of unannotated HOGs contained only *Berghia* sequences.

Out of a total of 24,762 transcripts that ended up in the single cell dataset, 48% (11891) were unannotated, and 52% annotated (12871). Within unannotated transcripts, 31% (3680) were shared between *Berghia* and at least one other species, and 69% (8211) were *Berghia* only. After removing genes with an adjusted p-value above 0.05, there were 3181 differentially expressed genes among all clusters. Forty percent (1279) of differentially expressed genes were unannotated, 39% (500) of which were shared between *Berghia* and at least 1 other species, and 61% (779) were from *Berghia* alone. Unannotated genes were expected for molluscs, where there is much less molecular data and functional characterization of these genes. Artifacts from the reference transcriptome assembly and annotation pipeline were also expected, and represent spurious sequences that could be chimeric, misassembled or only partly assembled and therefore not annotated. Such artifacts are unavoidable. However, we assume that artifacts would not be expected to appear in lists of differentially expressed genes, as sequenced reads are unlikely to be mapped to them.

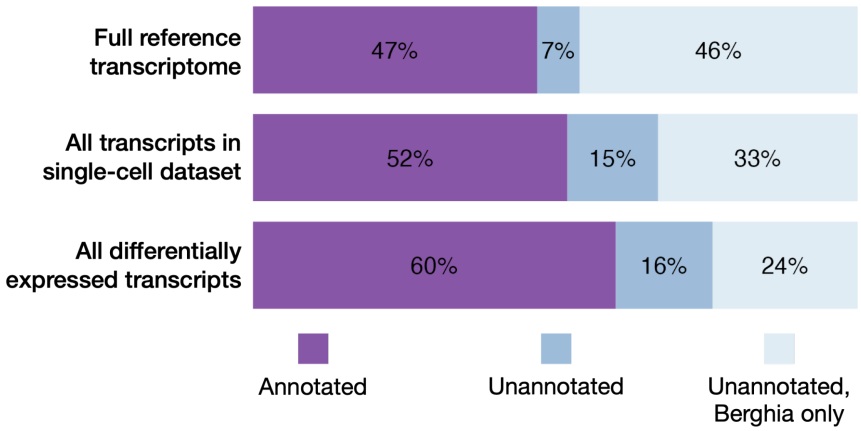

Figure 15: Stacked bar plots of the proportions of HOGs that were annotated, unannotated and shared between *Berghia* and at least one other species, and *Berghia*-specific for different subsets of the transcriptome. The threshold for differentially expressed genes was a FDR adjusted p-value of less than 0.05.

To localize mRNA for unannotated genes in the brain, we performed HCR on a small sample of unannotated, differentially expressed genes. As described previously, the gene *Bs19097* was found broadly expressed in putative neuronal clusters in the single cell dataset, and the expression pattern of this gene in most cells that were neurons (see Fig. 4E & F) supports the pattern found in the single cell atlas (see Fig. 3). *Tph*-expressing serotonergic neurons formed a very small but distinct cluster in the atlas, and the expression patterns for genes in these cells, including *Tph, Unc-4,* and *Scf46m3* were validated (see Fig. 13). Expression of an unannotated gene from the list of differentially expressed genes for serotonergic neurons, *Bs1707,* was restricted exclusively to *Tph*-expressing neurons, as expected for a top cluster marker gene (Fig. 16A, B). Another unannotated gene, *Bs4895* was differentially expressed in *rhg* neurons (Fig. 16C). Visualization of mRNA for this gene showed high, specific expression in neurons in the *rhg* (Fig. 16D). A small number of neurons outside of the *rhg* also express this gene, including a giant, unilateral, individually identifiable neuron in the right *pdg* (Fig. 16D). These validated examples, as well as the large percentage of unannotated, yet differentially expressed genes in the single cell atlas, support the idea that while unknown, these genes are important for neuron function and deserve further study.

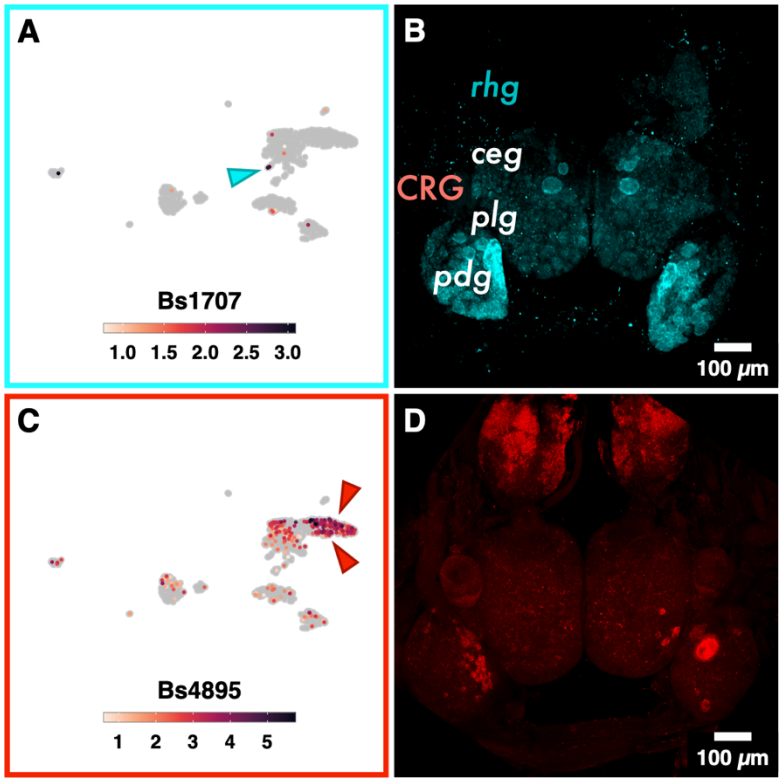

Figure 16: Differentially expressed, unannotated genes are expressed in a cluster-specific manner. A) Unannotated gene *Bs1707* was differentially expressed in the small cluster of *Tph+* neurons in the single cell dataset. A Z-projection of a fluorescence confocal image using HCR to label mRNA for *Bs1707* showed its expression was exclusive to the serotonergic, *Tph+* neurons in the brain. B) Unannotated gene *Bs4895* was differentially expressed in *rhg* clusters in the single cell dataset. A Z-projection of a fluorescence confocal image using HCR to label for *Bs4895* showed widespread, high expression in the *rhg.* However, there were also multiple, small, discrete groupings of *Bs4895+* neurons in the *plg* and *pdg,* including one giant neuron in the *pdg.*

Discussion

Individually identifiable neurons are a hallmark of gastropod head ganglia, including those of *Berghia.* The size, location, projections, physiological properties and gene expression are all measurable phenotypes that can be used to assign individual identities to neurons. Yet, the molecular and developmental mechanisms by which neurons gain their distinct identities in gastropods is unknown. Similarly unknown are most genes that together make up the final

mature molecular phenotypes for these neuron types. Furthermore, only a small percentage of the neuronal population has been identified due in part to the inefficiency of methods previously used to identify them. It is not known whether every neuron, or only a small subset, has an addressable identity. Moreover, the focus on individual neurons has completely ignored whether there is ganglionic organization that could be revealed by molecular signatures of large numbers of neurons.

Using a new study species, *Berghia stephanieae*, we created an annotated reference transcriptome and 1580 single cell transcriptomes from two sample types, the central ring ganglia (CRG), and the rhinophore ganglia (*rhg*). Standard clustering and differential gene expression analyses led to lists of candidate genes that were explored using multiplex *in-situ* hybridization chain reaction (HCR). We found that there are broad classes of neurons, some of which are regionally restricted and others of which are scattered throughout the brain. This approach allowed us to map the locations of neurons using small molecule neurotransmitters and/or neuropeptides without the concern about cross-reactivity of antibodies yielding false positives. The single-cell resolution of transcriptomic data also revealed candidate genes that weren't previously known from other transcriptomic analyses of gastropod nervous systems. The results yielded several new insights into important genes for neuronal cell type identities and the molecular organization of gastropod nervous systems.

Widespread distribution of glutamatergic and cholinergic neuronal classes

Neurons expressing markers for small molecule neurotransmitters (e.g., glutamate, acetylcholine, and GABA) were found in all the scRNAseq neuronal clusters. HCR for *Vglut* and *Chat* showed widespread distribution of neuronal somata in all ganglia, and of varying soma sizes. Thus, these two neuronal classes are large umbrellas containing high numbers of different neuronal cell types. Glutamate and acetylcholine are likely to play major roles in neural

circuits in *Berghia* as has been suggested by pharmacological studies in other nudibranchs (Sakurai and Katz 2017; Megalou, Brandon, and Frost 2009). Consistent with previous studies of GABA IHC which showed a more restricted distribution across neurons in nudibranchs (Gunaratne, Sakurai, and Katz 2014; Gunaratne and Katz 2016), *Gad* mRNA was found in a small number of neurons in the scRNAseq atlas data.

Serotonergic neurons form a distinct class with multiple neuronal cell types

In contrast to markers for glutamate, acetylcholine and GABA, markers for serotonergic neurons were highly restricted to a single UMAP cluster and the somata were found in specific locations in the *ceg* and *pdg*. This distribution of somata was known previously from serotonin IHC in other nudibranch species (James M. Newcomb, Fickbohm, and Katz 2006). Many of these neurons have been studied for their roles in motor behaviors in other gastropods (Joshua L. Lillvis and Katz 2013; J. L. Lillvis, Gunaratne, and Katz 2012; Getting, Lennard, and Hume 1980; Jing and Gillette 1999; Zhang et al. 2003; Yeoman et al. 1994).

Because they formed a discrete cluster in the scRNAseq atlas, we were able to look for differentially expressed genes that were specific to serotonergic neurons. Here, we found that all serotonergic neurons expressed *Unc-4*, but *Unc-4* expression was not restricted to those neurons. In contrast to our results from *Berghia*, *Unc-4* is primarily associated with cholinergic motor neurons in both *C. elegans* and *Drosophila (Pflugrad et al. 1997; Lacin et al. 2020)*). Thus, there has been a clear switch of association between *Unc-4* and cholinergic to serotonergic neurons in *Berghia*. This raises at least two potential evolutionary scenarios: either co-option of *Unc-4* for the specification of serotonergic neurons, or the switch of neurotransmitter phenotype for neurons specified by *Unc-4.* Because cholinergic neurons in *Berghia* are not also specified by *Unc-4*, the first scenario of co-option may be less likely, as it requires both a gain of association with *Unc-4* in serotonergic neurons and a loss of association

of *Unc-4* in cholinergic neurons. Therefore, an ancestral coding of neuronal type may have undergone a transmitter shift since the common ancestor of protostomes.

Different patterns for neuropeptide expression

We were able to recover evidence for expression of 40 of the 65 known molluscan neuropeptides, which was unexpected given the small total number of single cell transcriptomes in the dataset. High complexity in our small sample of neurons suggests that many neuropeptides may be expressed in many different neuron types rather than being restricted, for the most part, to a single neuronal class. More extensive surveying may find combinatorial expression of multiple neuropeptides in each neuron, seen in the giant ventral neuron that expressed at least three neuropeptides: *APGWamide*, *SCP* and *FCAP*. The survey of expression patterns for 8 neuropeptides showed relatively little overlap of sampled neuropeptides in the same neurons, again consistent with the high complexity of potential co-expression given the large number of expressed neuropeptides.

The expression of olfaction-associated genes, including nitric oxide synthase and soluble guanylate cyclase, show spatial organization in the rhinophore ganglia and is consistent with the hypothesized function of the rhinophores as distance chemoreceptors.

Neurons in two *rhg* clusters express nitric oxide synthase (*Nos*). Nitric oxide (NO) signaling is used by neurons in the olfactory centers of many animals, including molluscs like the snail *Lymnaea stagnalis(Gelperin 1994)*. As nudibranch rhinophores are thought to be distance chemoreceptors, expression of *Nos* in the *rhg* is consistent with that function. Outside of the *rhg, Nos* was also found in some neurons in the *ceg* and *plg*. This is a broader distribution than would be expected by previous studies using IHC or NADPH diaphorase staining in other nudibranchs (Hurst et al. 1999; Moroz and Gillette 1996; Newcomb and Watson 2001).

Soluble guanylate cyclase (*Sgc*) is known as a receptor for NO (Martin et al. 2005), and we found it was differentially expressed in the scRNAseq atlas in a separate cluster of *rhg* neurons than those expressing *Nos*. Multiplexed HCR for *Nos* and *Sgc* in the *rhg* revealed the spatial separation of *Nos* and *Sgc*-expressing populations of neurons. This spatial organization of *Nos*, *Pdf*, and *Sgc*-expressing neurons in the *rhg* hints at complex structural organization of the *rhg*, a ganglion that has received significantly less attention than other head ganglia. This complexity would not have been apparent without both the ability to detect differential gene expression between populations of neurons using high-throughput methods, and the ability to easily visualize the mRNA within those groups of neurons via HCR.

The expression of other olfaction-associated marker genes in the *rhg* is also consistent with the expected function of the rhinophores as distance chemoreceptors. One *Nos*-expressing *rhg* cluster in the scRNAseq atlas showed differential expression of the neuropeptide *Pigment dispersing factor* (*Pdf*). Consistent with the separation seen in the scRNAseq atlas data, multiplexed HCR labeling of *Nos* and *Pdf* found populations of *Nos*-expressing *rhg* neurons that were spatially segregated from those that expressed both *Nos* and *Pdf*. In the snail *Helix*, *Pdf* is expressed in multiple parts of the CRG, including the procerebrum, thought to be their olfactory center (Elekes and Nässel 1999). *Enterin* is also differentially expressed in *rhg* clusters in the scRNAseq atlas. In the slug *Limax*, *enterin* is expressed in their olfactory centers, the procerebrum and tentacular ganglia. Ectopic application of *enterin* modulates local field potential oscillations in these ganglia (Matsuo et al. 2020).

Expression of transcription factors also reveals molecular organization at different spatial scales within the head ganglia

There are regional and ganglionic expression differences in transcription factors and neuropeptides. Expression of *Six3/6*, a member of the *Six/sine oculis* family of homeobox containing transcription factors, is restricted to the anterior-most major head ganglia (the *ceg* and *rhg*). This expression pattern is shared across bilaterians, including mammals (Conte, Morcillo, and Bovolenta 2005), indicative of conservation of an ancestral role for *Six3/6* in delineating anterior portions of nervous systems.

The activity of transcription factors (TF) is usually associated with developmental processes in animals, but they also act as "terminal selectors" whose expression maintains mature neuronal phenotypes (Hobert and Kratsios 2019). Many transcription factors were found in the single cell transcriptomes. Those TFs associated with neuroblasts and newly differentiated neurons like *sox2, sox6,* and *scratch* were differentially and specifically expressed in one cluster in the scRNA-seq atlas. It is not yet clear whether there are neuroblasts in the brain itself—neurogenesis zones in other gastropods are in the body wall epithelium of the animal, and postmitotic neurons migrate into the GRG (Jacob 1984). Both *Six3/6* and *Delta* were differentially expressed in the glutamatergic *Sgc rhg* neuron cluster of the scRNAseq atlas. Multiplexed HCR showed that they were often co-expressed in *rhg* neurons. Yet *Six3/6* and *Delta* expression was not restricted only to the *rhg,* further supporting their role as a broad neuronal class marker.

The prevalence of unannotated genes.

Research in other organisms has homed in on "conserved hypothetical proteins" (Galperin and Koonin 2004) as important foci for functional research. The importance of looking at these types of unannotated genes was highlighted by this project; unannotated genes made up ~40% of genes that were differentially expressed between clusters, both neuronal and non-neuronal. While we did not specifically analyze the lineage conservation of unannotated genes in our

dataset, we explicitly considered the conservation of *Berghia* sequences with at least one other gastropod as part of the filtering of the reference transcriptome.

The expression of two such markers were visualized using HCR and the expression patterns corresponded specifically to their respective clusters. For example, *Bs1707* is an unannotated gene that is present in all nudibranch transcriptomes, but only expressed in serotonergic neurons. Another unannotated gene, *Bs4895*, is highly expressed in *rhg* neurons and in a very restricted set of *pdg* neurons. While not a cluster-specific marker, unannotated gene *Bs19097* was widely expressed in putative neuronal clusters and labeled neurons on all ganglia. The exact nature of *Bs19097* remains unknown, its distribution establishes it as a pan-neuronal marker like *elav*. In addition, we found that *7B2*, which has been described as a gene expressed in all neurons in mouse, was also broadly expressed in *Berghia* neurons. The expression pattern of *Bs19097* also matched the pan-neuronal expression of 7B2.

The molecular genetics of gastropods has not been well characterized because of the difficulty in genetic manipulations to test gene function in these animals. Some unannotated genes were expected based on the number of “hypothetical proteins” available in molluscan genomes, and recent scRNAseq studies have also described unannotated genes as markers for specific populations of neurons (Albertin et al. 2015; Styfhals et al. 2022; Songco-Casey et al. 2022). The great number of unannotated genes shows how much there is to learn about these molecules and their functions in the nervous system.

Gene expression profiles of individual neurons

We expected to find that because individual neurons can be identified in gastropods (Leonard 2000; Katz and Quinlan 2019; Croll 1987), they would have clear molecular signatures. However, the methodology used here was biased against finding rare cells that did not share

gene expression profile similarities with many other cells. That said, we were able to show that a neuron that was visually identifiable based on soma size and position, the giant ventral peptidergic neuron, did have a particular signature. We found this neuron expressed at least three neuropeptides and *Chat*. This suggests that intersectional transcriptomics might provide gene expression fingerprints for each neuron.

Functional implications of gene expression

Suites of genes that are co-expressed in neuronal types that may be shared across animals were identified in the *Berghia* single cell dataset. Based on the known bilaterian molecular signature for mechanosensory-related neurons, the co-expression of *Brn3* and *Vglut* that was found in *Berghia* suggests that these cells may be part of mechanosensory circuits, as their potential homologs are known to be in *Lymnaea* and *Aplysia* (Brunet et al. 1991; Nomaksteinsky et al. 2013). We did not find the extensive co-expression of *Brn3* and *Sensorin-A* in S-cells/J,K c cluster cells seen in other gastropods (Nomaksteinsky et al. 2013). Instead, a few cells adjacent to the S-cells express *Brn3*. There were a small number of neurons that did co-express these genes, but they were located at the lateral edges of the ganglia.

Non-neuronal cells

Four types of glial cells were previously identified in other gastropods based on immunoreactivity to glial fibrillary acid protein (Santos et al. 2002). We identified three clusters of glial cells in the scRNAseq data and two additional clusters of non-neuronal cells, which have markers for endothelial cells and fibroblasts. Gastropod ganglia are surrounded by a connective tissue sheath. Some of those cells may be included in the five non-neuronal clusters. Future *in situ* labeling will be able to localize these genes to specific cell types in the ganglia.

Summary

Molluscs, and specifically gastropods, have been important study systems in neuroscience for decades from a cell and circuit perspective. This project shows that new egalitarian molecular tools can be applied to a gastropod mollusc like *Berghia* to accelerate our understanding of the molecular bases for neuronal identity and function in gastropods and other molluscs. The role for gastropods in modern neuroscience can be expanded and provides an important phylogenetic data point to understand general principles of nervous systems.

Methods

Berghia husbandry

Adult *Berghia* were originally purchased from online suppliers Salty Underground and Reef Town. They were housed in 5-gallon glass tanks with ~10 individuals. Multiple sea anemones (*Exaptasia diaphana*) were provided to each tank every other day as food. Colonies of *Exaptasia* were raised in 10-gallon tanks with continuously running filters and were fed every other day with freshly hatched *Artemia* nauplii, which were hatched every 2 days by placing ~2.5g of freeze dried *Artemia* eggs into an aeration chamber with fresh artificial seawater (Instant Ocean). All animals were kept in the same room, which was held at 26℃ to mimic conditions in *Berghia*'s ambient environment in the Florida Keys, USA. The room that housed all the animals was kept on a constant 12:12 light: dark cycle. Larger (~1.5cm), egg-laying adults were chosen from random tanks for dissection.

Single neuron RNA sequencing

Creating single neuron suspensions

Brains were dissected and treated in a mixture of 2% w/v pronase (Sigma-Aldrich, St. Louis, MO) and 0.2% w/v Liberase (Sigma-Aldrich, St. Louis, MO) in calcium-, magnesium-free artificial seawater (CMFSW) to digest the ganglionic sheath. Then, the rhinophore ganglia were removed with scissors from the CRG at the connective. A total of 18 pairs of *rhg* and 20 CRG (B) samples were recovered. Ganglia were pooled to create one sample for each type of ganglion. The two samples were processed separately because of a large difference in the average size of the neurons. Most of the *rhg* neurons were less than 10μm in diameter, whereas CRG neurons ranged from 10-60μm in diameter.

Each sample was triturated in a 400μL of CMFSW until a single-cell suspension was achieved with minimal cell lumps. CRG samples were mixed for 2 minutes with regular-bore P200 tip at a quick pace, 1 minute with wide-bore P200 tip at a slower pace, and 1 minute with regular-bore P200 tip at the same slow pace. *Rhg* samples were mixed for 4 minutes with regular-bore P200 tip at a quick pace. Cell suspensions were filtered through a 400μL layer of 4% bovine serum albumin (BSA) in CMFSW at 4◦C. The suspensions were then centrifuged in a swing bucket centrifuge at 4°C for 10 minutes at 100 x g for the CRG sample and for 6 minutes at 400 x g for the *rhg* sample.

After centrifugation, the cell pellets were resuspended in 1.5mL round bottom tubes (Eppendorf DNA LoBind, Eppendorf, Enfield, CT) with 400μL of CMFSW and fixed in 1.6mL of 100% methanol. Precipitants form at this step from the salt in CMFSW. We incubated tubes for 10 minutes at -20°C and centrifuged them in the swing bucket centrifuge for 5 minutes at 4°C and

500 x g. Two mL of 0.5% w/v BSA in 1X phosphate-buffered saline (PBS) were added to dissolve the salt. The suspensions were centrifuged again as above. 400µL of 0.5% w/v BSA in 1X PBS was added first then 1600µL of 100% methanol were added drop by drop to fix the cells. The tubes were stored at -20°C overnight, or for several weeks while other samples were collected.

Single neuron library preparation and high-throughput sequencing

Cell suspensions were sent to The Bauer Core Facility at Harvard University for library preparation using the 10x Genomics Chromium platform. They also sequenced the single cell libraries on an Illumina NovaSeq.

Bulk brain transcriptome library preparation and sequencing

Berghia brains (CRG plus *rhg*) were dissected and put into lysis buffer from the Smart-Seq4 kit (Takara Bio USA Inc., San Jose, CA) and stored at -20°. RNA was extracted from the brains and library prep performed following manufacturer's protocols. We used magnetic beads (beads info) to enrich our samples for mRNA before proceeding to library preparation. Prepared libraries yield was quantified using Qubit (info) and library quality using a Bioanalyzer (info). Some samples could not be quantified because the concentration was too low, but Bioanalyzer traces suggested a quality library, and so these samples were kept in the dataset. Bulk transcriptome sequencing was performed by the Genomics Resource Facility at the University of Massachusetts-Amherst using an Illumina Next-Seq 500.

Brain transcriptome assembly, phylogenetic validation of transcripts and annotation

The raw reads of the brain samples as well as samples from tissues across the body of *Berghia* were concatenated and put into the Oyster River Protocol (MacManes 2018) pipeline for assembly. This pipeline uses multiple assemblers and multiple k-mers. This is necessary because different algorithms assemble true transcripts that are missed by others (Smith-Unna et al. 2016). The pipeline uses trimmomatic (Bolger, Lohse, and Usadel 2014) to trim reads to remove adapter sequences and low-quality reads. The cleaned reads are assembled using Trinity (Grabherr et al. 2011), Oases (Schulz et al. 2012) and SOAPdenovo (Xie et al. 2014). Orthofinder2 (Emms and Kelly 2018) has been modified to concatenate sequences across transcriptomes from different assemblers to reduce duplicate sequences.

We used a phylogenetic approach to further consolidate the *Berghia* transcriptome and clear out spurious transcripts. We assumed that if a homologous transcript could be found in at least 2 other gastropod species, that it is a real transcript. Orthofinder2 was used to create a list of Berghia transcripts that met those criteria. Orthofinder2 takes transcriptomes from multiple species and attempts to assign transcripts to hierarchical orthogroups (HOGs). Orthogroups are first created using diamond (Buchfink, Reuter, and Drost 2021) to search and group transcripts from each species using sequence similarity, MAFFT (Katoh and Standley 2013) to align the sequences per orthogroup and FastTree (Price, Dehal, and Arkin 2010) to build a gene tree for each orthogroup. Orthofinder2 then uses the outputs of this first step to find single copy orthologs and create a species tree. Finally, Orthofinder2 performs a gene-species tree reconciliation for each orthogroups' gene tree to identify the duplications and losses of orthologs

and paralogs that can confuse proper assignment of orthology and to place these events on each gene tree.

The output includes a list of each orthogroup, now put into a unique HOG after the gene-species tree reconciliation, and the transcripts from each species that are putative orthologs. We gave Orthofinder2 the coding sequence transcriptomes from gastropod species with genomes, such as *Aplysia*, *Lottia* and *Pomacea*. We also included our Berghia transcriptomes as well as brain transcriptomes from multiple other nudibranch species, including *Melibe leonina*, *Dendronotus iris*, and *Hermissenda opalescens* (formerly identified as a sample from *Hermissenda crassicornis*). Finally, we included sequences for neuropeptides known from other lophotrochozoans that have been verified in the marine worm *Platynereis dumerili*. Any HOG that did not have a transcript from *Berghia*, or that had transcripts from fewer than two other species of gastropods were excluded from downstream analyses.

The *Berghia* transcriptome from ORP was annotated using EnTAP (Hart et al. 2020), and Trinotate (Ghaffari et al. 2014). These annotations, along with those from *Aplysia*, *Pomacea*, and *Platynereis* were then assigned to HOGs, which could then be mapped onto transcripts from *Berghia*. We found this approach necessary because we found many unannotated transcripts were differentially expressed between neurons using our single cell transcriptome data. It was difficult to know whether these represented true transcripts that do not share any similarity with annotated sequences, or chimeric or artifactual transcripts from assembly errors.

Final HOGs were selected based on the following criteria: 1) they include a sequence from *Berghia* and at least one other species or 2) the *Berghia* sequence was predicted as a complete peptide at least 30 amino acids long. While these permissive criteria may keep some sequences that are spurious or artifacts of assembly, we included them because we know that many

neuropeptides are fewer than 100 amino acids. Our expectation is that reads from single cell transcriptomes should not map well to spurious sequences. For similar reasons, we kept sequences even if they could not be annotated using any publicly available database.

Single cell gene expression clustering analysis and differential gene expression analysis

Raw reads for each sample type were processed for quality and adapters trimmed using HTStream (Petersen et al. 2015)https://github.com/s4hts/HTStream(Petersen et al. 2015) with default settings. kallisto (Bray et al. 2016) was used to pseudo-map reads onto our reference transcriptome and bustools (Melsted et al. 2021) to generate gene counts per cell. After mapping, the outputs of bustools were imported into R using the bustools kbk command. Kneeplots were used to exclude empty droplets and those containing ambient RNA. A standard Seurat (Hao et al. 2021) normalization and analysis pipeline was used on the single cell transcriptomes. Briefly, each sample type was imported separately, and genes that were not expressed in at least 3 cells, and cells expressing fewer than 200 genes were excluded. The data were merged while keeping track of the origins of data for each cell and checked for batch effects looking at the number of UMIs and genes in each sample. There was no evidence for batch effects, so all downstream analyses were performed on both samples combined. After removing cells that failed to meet the above criteria, counts for each gene were normalized by the total expression in each cell, scaled by multiplying by 10,000, and finally log-transformed. The FindVariableFeatures command was used to identify the 2000 most highly variable genes.

After running a principal component (PC) analysis, the first 50 PCs were included in dimensionality reductions using tSNE (t-distributed Stochastic Neighborhood Embedding,

resolution 3) and UMAP (Uniform Manifold Approximation and Projection) methods as implemented in Seurat. To select the resolution used in tSNE, Clustree (Zappia and Oshlack 2018) was used to look at the effect of changing tSNE resolution on the stability of clusters. The highest resolution value showed only a small amount of instability compared to the next smallest value (see Supplementary Figure 2). We looked for the most highly differentially expressed genes between clusters using the FindMarker command in Seurat, using MAST (Finak et al. 2015; Dal Molin, Baruzzo, and Di Camillo 2017) to estimate differential expression. Clusters without meaningful differences in genes that were differentially expressed were collapsed together using the Clustree results. There were 14 clusters in the final analysis. We used the FeaturePlot and DoHeatmap commands in Seurat to visualize gene expression. We also used the R package nebulosa (Alquicira-Hernandez and Powell 2021) to estimate the kernel density of expression for genes of interest. All code for running this analysis is available in the Supplementary Methods.

Creating DNA probes for *in-situ* Hybridization Chain Reaction (HCR)

BLASTP was used with queries from *Aplysia* and *Lymnaea* to look for candidate genes in the reference transcriptome. ExPAsy translate (https://web.expasy.org/translate/) was used to translate the nucleotide sequence into amino acids for possible reading frames, to determine whether the sequence was the sense or anti-sense strand. If the sequence was anti-sense, the reverse complement of the sequence was identified (https://www.bioinformatics.org/sms/rev_comp.html). The longest predicted peptide was selected and used BLAST on NCBI databases to verify that the best hits for the predicted peptide matched were like those of the nucleotide sequence where possible. The best BLAST hits needed to be from molluscs and have the same annotation where annotations were

available. Sequences for the probe sets for each gene were made using the HCRProbeMaker script (Kuehn et al. 2021) with the sense strand, based on the requirements necessary for HCR found in (Choi et al. 2018). This script found a user-selected number of probe pairs that would bind to the target mRNA sequence with 2 base pairs in between and added one of 5 initiator sequences to each partner that are necessary for the initiation of the fluorescent hybridization chain reaction. Probe set oligos from this script were synthesized by IDT (Integrated DNA Technologies, Coralville, IA, USA) and the lyophilized probes were rehydrated with enough TE buffer to end up with a 50 picomolar stock concentration. Probe sets for choline acetyltransferase (54 probe pairs) and APGWamide (20 probe pairs), as well as the fluorescent hairpins were purchased from Molecular Instruments (Los Angeles, CA).

Labeling transcripts using HCR

Hybridization chain reaction reagents were made using the recipes from (Choi et al. 2018), substituting urea one-for-one instead of formamide. This substitution has been tested for traditional colormetric *in-situ* hybridizations and shown to be equally effective (Sinigaglia et al. 2018). Both the formamide and urea formulations were tested and no differences in HCR results detected, and so urea-based hybridization solutions were used for all HCR. Samples were fixed for at least 2 hours (at room temperature) to overnight (at 4deg C) in 4% paraformaldehyde (Electron Microscopy Sciences, Hatfield, PA) in artificial sea water. After fixation, samples were washed briefly in phosphate-buffered saline (PBS, ThermoFisher Scientific, Agawam, MA) and then dehydrated through a series from 100% PBS to 100% methanol. Samples in methanol were stored at least overnight at -20deg C for up to 1 month.

On the first day of HCR processing, samples were rehydrated in series into 100% 5X sodium citrate saline (SSC, diluted from 20X stock solution, Thermofisher Scientific, Agawam, MA) and

0.1% Tween-20 added (SSCT). They sat in 5X SSCT at room temperature for at least 15 minutes before being moved to a tube containing ~200uL of hybridization buffer in a heat block set to 37° C to equilibrate for at least 30 minutes. During this time, probe sets for each gene were thawed at room temperature, and a small volume was mixed into 100uL of fresh hybridization buffer. The concentration of probe needed for successful labeling varied between probe sets, from 0.1 picomolar to 1 picomolar. After equilibration in hybridization buffer, as much of the used buffer was removed from the tube as possible while keeping the sample submerged. The probe-hybridization buffer mixture was then added to the tube, and the sample incubated overnight at 37° C.

The following day, the samples were washed in hybridization wash twice for 5 minutes, and twice for 30 minutes at 37° C. During the final 30-minute wash, the appropriate Alexa-dye-tagged hairpins for each initiator were thawed at room temperature in the dark. Haiprins with Alexa 488, 546, 594 or 647 dyes were used to multiplex labeling of 2-3 genes per sample. 2 uL of each hairpin pair per initiator were used in a final volume of 100uL amplification buffer. Each hairpin solution was aliquoted into a 0.2mL PCR strip tube. Hairpins were then “snapped” to linearize them by heating at 95° C for 90 seconds followed by 30 minutes of cooling at room temperature in the dark. All hairpins were then added to the appropriate volume of amplification buffer to a final volume of 100uL. The hybridization chain reaction occurred in the amplification buffer either overnight or for 2 overnights. The length of amplification time was determined empirically, but in general, highly expressed genes needed less amplification time, and the lowest expressed genes needed the longest time.

After amplification, the samples were washed in 5x SSCT once. The nuclei were labeled using 1uL 300uM DAPI : 1000uL 5x SSCT, rotating in the dark for 1 hour. Brains were mounted onto long coverglass using 2 small strips of double-sided tape (Scotch) as spacers and to attach the

small coverglass. Either Vectashield Vibrance (Vector Laboratories) or a fructose-glycerol solution (Elagoz et al. 2022) was used to clear and mount the samples for confocal imaging.

Confocal imaging of multiplexed HCR samples and image processing

Fluorescent confocal images were taken at 20x using the Nikon A1R-25 or A1R-18 at the Light Microscopy Facility at the University of Massachusetts-Amherst. Images were processed in ImageJ to rotate the image as needed, normalize intensity, adjust brightness and contrast, and create scale bars.

References

Albertin, Caroline B., Oleg Simakov, Therese Mitros, Z. Yan Wang, Judit R. Pungor, Eric Edsinger-Gonzales, Sydney Brenner, Clifton W. Ragsdale, and Daniel S. Rokhsar. 2015. "The Octopus Genome and the Evolution of Cephalopod Neural and Morphological Novelties." *Nature* 524 (7564): 220–24.

Alquicira-Hernandez, Jose, and Joseph E. Powell. 2021. "Nebulosa Recovers Single Cell Gene Expression Signals by Kernel Density Estimation." *Bioinformatics* , January. https://doi.org/10.1093/bioinformatics/btab003.

Arey, L. B. 1918. "The Multiple Sensory Activities of the so-Called Rhinophore of Nudibranchs." *American Journal of Physiology-Legacy Content*. https://journals.physiology.org/doi/pdf/10.1152/ajplegacy.1918.46.5.526.

Asprer, Joanna S. T., Bora Lee, Chia-Shan Wu, Tegy Vadakkan, Mary E. Dickinson, Hui-Chen Lu, and Soo-Kyung Lee. 2011. "LMO4 Functions as a Co-Activator of Neurogenin 2 in the Developing Cortex." *Development* 138 (13): 2823–32.

Bernier, G., F. Panitz, X. Zhou, T. Hollemann, P. Gruss, and T. Pieler. 2000. "Expanded Retina Territory by Midbrain Transformation upon Overexpression of Six6 (Optx2) in Xenopus Embryos." *Mechanisms of Development* 93 (1-2): 59–69.

Bettenhausen, B., M. Hrabě de Angelis, D. Simon, J. L. Guénet, and A. Gossler. 1995. "Transient and Restricted Expression during Mouse Embryogenesis of Dll1, a Murine Gene Closely Related to Drosophila Delta." *Development* 121 (8): 2407–18.

Bolger, Anthony M., Marc Lohse, and Bjoern Usadel. 2014. "Trimmomatic: A Flexible Trimmer for Illumina Sequence Data." *Bioinformatics* 30 (15): 2114–20.

Bray, Nicolas L., Harold Pimentel, Páll Melsted, and Lior Pachter. 2016. "Near-Optimal Probabilistic RNA-seq Quantification." *Nature Biotechnology* 34 (5): 525–27.

Brunet Avalos, Clarisse, G. Larisa Maier, Rémy Bruggmann, and Simon G. Sprecher. 2019. "Single Cell Transcriptome Atlas of the Drosophila Larval Brain." *eLife* 8 (November). https://doi.org/10.7554/eLife.50354.

Brunet, J. F., E. Shapiro, S. A. Foster, E. R. Kandel, and Y. Iino. 1991. "Identification of a

Peptide Specific for Aplysia Sensory Neurons by PCR-based Differential Screening." *Science* 252 (5007): 856–59.
Bryant, Donald M., Kimberly Johnson, Tia DiTommaso, Timothy Tickle, Matthew Brian Couger, Duygu Payzin-Dogru, Tae J. Lee, et al. 2017. "A Tissue-Mapped Axolotl De Novo Transcriptome Enables Identification of Limb Regeneration Factors." *Cell Reports* 18 (3): 762–76.
Buchfink, Benjamin, Klaus Reuter, and Hajk-Georg Drost. 2021. "Sensitive Protein Alignments at Tree-of-Life Scale Using DIAMOND." *Nature Methods* 18 (4): 366–68.
Buescher, Marita, Fook Sion Hing, and William Chia. 2002. "Formation of Neuroblasts in the Embryonic Central Nervous System of Drosophila Melanogaster Is Controlled by SoxNeuro." *Development* 129 (18): 4193–4203.
Chao, Michael Y., Jonah Larkins-Ford, Tim M. Tucey, and Anne C. Hart. 2005. "Lin-12 Notch Functions in the Adult Nervous System of C. Elegans." *BMC Neuroscience* 6 (July): 45.
Chitnis, A., D. Henrique, J. Lewis, D. Ish-Horowicz, and C. Kintner. 1995. "Primary Neurogenesis in Xenopus Embryos Regulated by a Homologue of the Drosophila Neurogenic Gene Delta." *Nature* 375 (6534): 761–66.
Choi, Harry M. T., Maayan Schwarzkopf, Mark E. Fornace, Aneesh Acharya, Georgios Artavanis, Johannes Stegmaier, Alexandre Cunha, and Niles A. Pierce. 2018. "Third-Generation in Situ Hybridization Chain Reaction: Multiplexed, Quantitative, Sensitive, Versatile, Robust." *Development* 145 (12). https://doi.org/10.1242/dev.165753.
Conte, Ivan, Julian Morcillo, and Paola Bovolenta. 2005. "Comparative Analysis of Six 3 and Six 6 Distribution in the Developing and Adult Mouse Brain." *Developmental Dynamics: An Official Publication of the American Association of Anatomists* 234 (3): 718–25.
Cornbrooks, Carson, Christin Bland, Darren W. Williams, James W. Truman, and Matthew D. Rand. 2007. "Delta Expression in Post-Mitotic Neurons Identifies Distinct Subsets of Adult-Specific Lineages in Drosophila." *Developmental Neurobiology* 67 (1): 23–38.
Croll, Roger P. 1987. "Identified Neurons and Cellular Homologies." In *Nervous Systems in Invertebrates*, edited by M. A. Ali, 41–59. Boston, MA: Springer US.
———. 2001. "Catecholamine-Containing Cells in the Central Nervous System and Periphery of Aplysia Californica." *The Journal of Comparative Neurology* 441 (2): 91–105.
Croll, R. P. 1987. "Identified Neurons and Cellular Homologies." *Nervous Systems in Invertebrates*. https://link.springer.com/chapter/10.1007/978-1-4613-1955-9_4.
Cummins, Scott F., and Russell C. Wyeth. 2014. "Olfaction in Gastropods." *Neuroecology and Neuroethology in Molluscs: The Interface between Behaviour and Environment* 1: 45–72.
Dal Molin, Alessandra, Giacomo Baruzzo, and Barbara Di Camillo. 2017. "Single-Cell RNA-Sequencing: Assessment of Differential Expression Analysis Methods." *Frontiers in Genetics* 8 (May): 62.
De Oliveira, A. L., A. Calcino, and A. Wanninger. 2019. "Extensive Conservation of the Proneuropeptide and Peptide Prohormone Complement in Mollusks." *Scientific Reports* 9 (1): 4846.
D'Este, Loredana, Arianna Casini, Shin Kimura, Jean-Pierre Bellier, Etsuro Ito, Hiroshi Kimura, and Tindaro G. Renda. 2011. "Immunohistochemical Demonstration of Cholinergic Structures in Central Ganglia of the Slug (Limax Maximus, Limax Valentianus)." *Neurochemistry International* 58 (5): 605–11.
Elagoz, Ali M., Ruth Styfhals, Sofia Maccuro, Luca Masin, Lieve Moons, and Eve Seuntjens. 2022. "Optimization of Whole Mount RNA Multiplexed in Situ Hybridization Chain Reaction With Immunohistochemistry, Clearing and Imaging to Visualize Octopus Embryonic Neurogenesis." *Frontiers in Physiology* 13 (May): 882413.
Elekes, K., and D. R. Nässel. 1999. "Pigment-Dispersing Hormone-like Immunoreactive Neurons in the Central Nervous System of the Gastropods, Helix Pomatia and Lymnaea Stagnalis." *Cell and Tissue Research* 295 (2): 339–48.

Emms, David M., and Steven Kelly. 2018. “OrthoFinder2: Fast and Accurate Phylogenomic Orthology Analysis from Gene Sequences.” https://www.biorxiv.org/content/early/2018/11/08/466201.

Eng, Lawrence F., Roopa S. Ghirnikar, and Yuen L. Lee. 2000. “Glial Fibrillary Acidic Protein: GFAP-Thirty-One Years (1969–2000).” *Neurochemical Research* 25 (9): 1439–51.

Eng, L. F. 1985. “Glial Fibrillary Acidic Protein (GFAP): The Major Protein of Glial Intermediate Filaments in Differentiated Astrocytes.” *Journal of Neuroimmunology* 8 (4-6): 203–14.

Finak, Greg, Andrew McDavid, Masanao Yajima, Jingyuan Deng, Vivian Gersuk, Alex K. Shalek, Chloe K. Slichter, et al. 2015. “MAST: A Flexible Statistical Framework for Assessing Transcriptional Changes and Characterizing Heterogeneity in Single-Cell RNA Sequencing Data.” *Genome Biology* 16 (December): 278.

Galperin, Michael Y., and Eugene V. Koonin. 2004. “‘Conserved Hypothetical’ Proteins: Prioritization of Targets for Experimental Study.” *Nucleic Acids Research* 32 (18): 5452–63.

Gavriouchkina, Daria, Yongkai Tan, Fabienne Ziadi-Künzli, Yuko Hasegawa, Laura Piovani, Lin Zhang, Chikatoshi Sugimoto, Nicholas Luscombe, Ferdinand Marlétaz, and Daniel S. Rokhsar. 2022. “A Single-Cell Atlas of Bobtail Squid Visual and Nervous System Highlights Molecular Principles of Convergent Evolution.” *bioRxiv*. https://doi.org/10.1101/2022.05.26.490366.

Gelperin, A. 1994. “Nitric Oxide Mediates Network Oscillations of Olfactory Interneurons in a Terrestrial Mollusc.” *Nature* 369 (6475): 61–63.

Getting, P. A., P. R. Lennard, and R. I. Hume. 1980. “Central Pattern Generator Mediating Swimming in Tritonia. I. Identification and Synaptic Interactions.” *Journal of Neurophysiology* 44 (1): 151–64.

Ghaffari, Noushin, Alejandro Sanchez-Flores, Ryan Doan, Karina D. Garcia-Orozco, Patricia L. Chen, Adrian Ochoa-Leyva, Alonso A. Lopez-Zavala, et al. 2014. “Novel Transcriptome Assembly and Improved Annotation of the Whiteleg Shrimp (Litopenaeus Vannamei), a Dominant Crustacean in Global Seafood Mariculture.” *Scientific Reports* 4 (November): 7081.

Gold, Katrina S., and Andrea H. Brand. 2014. “Optix Defines a Neuroepithelial Compartment in the Optic Lobe of the Drosophila Brain.” *Neural Development* 9 (July): 18.

González, Roxana, Daniel González, Felipe Stambuk, Felipe Ramírez, Fanny Guzmán, Luis Mercado, Rodrigo Rojas, Carlos Henríquez, Katherina Brokordt, and Paulina Schmitt. 2022. “A G-Type Lysozyme from the Scallop Argopecten Purpuratus Participates in the Immune Response and in the Stability of the Hemolymph Microbiota.” *Fish & Shellfish Immunology* 123 (April): 324–34.

Grabherr, Manfred G., Brian J. Haas, Moran Yassour, Joshua Z. Levin, Dawn A. Thompson, Ido Amit, Xian Adiconis, et al. 2011. “Full-Length Transcriptome Assembly from RNA-Seq Data without a Reference Genome.” *Nature Biotechnology* 29 (7): 644–52.

Gunaratne, Charuni A., and Paul S. Katz. 2016. “Comparative Mapping of GABA-Immunoreactive Neurons in the Buccal Ganglia of Nudipleura Molluscs.” *The Journal of Comparative Neurology* 524 (6): 1181–92.

Gunaratne, Charuni A., Akira Sakurai, and Paul S. Katz. 2014. “Comparative Mapping of GABA-Immunoreactive Neurons in the Central Nervous Systems of Nudibranch Molluscs.” *The Journal of Comparative Neurology* 522 (4): 794–810.

Halter, D. A., J. Urban, C. Rickert, S. S. Ner, K. Ito, A. A. Travers, and G. M. Technau. 1995. “The Homeobox Gene Repo Is Required for the Differentiation and Maintenance of Glia Function in the Embryonic Nervous System of Drosophila Melanogaster.” *Development* 121 (2): 317–32.

Hao, Yuhan, Stephanie Hao, Erica Andersen-Nissen, William M. Mauck 3rd, Shiwei Zheng, Andrew Butler, Maddie J. Lee, et al. 2021. “Integrated Analysis of Multimodal Single-Cell Data.” *Cell* 184 (13): 3573–87.e29.

Hart, Alexander J., Samuel Ginzburg, Muyang Sam Xu, Cera R. Fisher, Nasim Rahmatpour, Jeffry B. Mitton, Robin Paul, and Jill L. Wegrzyn. 2020. “EnTAP: Bringing Faster and Smarter Functional Annotation to Non-Model Eukaryotic Transcriptomes.” *Molecular Ecology Resources* 20 (2): 591–604.

Heldman, E., Y. Grossman, T. P. Jerussi, and D. L. Alkon. 1979. “Cholinergic Features of Photoreceptor Synapses in Hermissenda.” *Journal of Neurophysiology* 42 (1 Pt 1): 153–65.

Henrique, D., J. Adam, A. Myat, A. Chitnis, J. Lewis, and D. Ish-Horowicz. 1995. “Expression of a Delta Homologue in Prospective Neurons in the Chick.” *Nature* 375 (6534): 787–90.

Hobert, Oliver, and Paschalis Kratsios. 2019. “Neuronal Identity Control by Terminal Selectors in Worms, Flies, and Chordates.” *Current Opinion in Neurobiology* 56 (June): 97–105.

Hurst, W. J., L. L. Moroz, M. U. Gillette, and R. Gillette. 1999. “Nitric Oxide Synthase Imunolabeling in the Molluscan CNS and Peripheral Tissues.” *Biochemical and Biophysical Research Communications* 262 (2): 545–48.

Hwang, J. R., D. E. Siekhaus, R. S. Fuller, P. H. Taghert, and I. Lindberg. 2000. “Interaction of Drosophila Melanogaster Prohormone Convertase 2 and 7B2. Insect Cell-Specific Processing and Secretion.” *The Journal of Biological Chemistry* 275 (23): 17886–93.

Irwin, David M. 2014. “Evolution of the Vertebrate Goose-Type Lysozyme Gene Family.” *BMC Evolutionary Biology* 14 (August): 188.

Irwin, David M., and Zhiyuan Gong. 2003. “Molecular Evolution of Vertebrate Goose-Type Lysozyme Genes.” *Journal of Molecular Evolution* 56 (2): 234–42.

Ishizawa, Kota, Hiroshi Kubo, Mitsuhiro Yamada, Seiichi Kobayashi, Takashi Suzuki, Shinya Mizuno, Toshikazu Nakamura, and Hidetada Sasaki. 2004. “Hepatocyte Growth Factor Induces Angiogenesis in Injured Lungs through Mobilizing Endothelial Progenitor Cells.” *Biochemical and Biophysical Research Communications* 324 (1): 276–80.

Itoh, Yasuhiro, Yasunobu Moriyama, Tsuyoshi Hasegawa, Takaho A. Endo, Tetsuro Toyoda, and Yukiko Gotoh. 2013. “Scratch Regulates Neuronal Migration Onset via an Epithelial-Mesenchymal Transition–like Mechanism.” *Nature Neuroscience* 16 (4): 416–25.

Jacob, M. H. 1984. “Neurogenesis in Aplysia Californica Resembles Nervous System Formation in Vertebrates.” *The Journal of Neuroscience: The Official Journal of the Society for Neuroscience* 4 (5): 1225–39.

Jayadev, Ranjay, and David R. Sherwood. 2017. “Basement Membranes.” *Current Biology: CB* 27 (6): R207–11.

Jing, J., and R. Gillette. 1999. “Central Pattern Generator for Escape Swimming in the Notaspid Sea Slug Pleurobranchaea Californica.” *Journal of Neurophysiology* 81 (2): 654–67.

Jung, W., E. Castren, M. Odenthal, G. F. Vande Woude, T. Ishii, H. P. Dienes, D. Lindholm, and P. Schirmacher. 1994. “Expression and Functional Interaction of Hepatocyte Growth Factor-Scatter Factor and Its Receptor c-Met in Mammalian Brain.” *The Journal of Cell Biology* 126 (2): 485–94.

Katoh, Kazutaka, and Daron M. Standley. 2013. “MAFFT Multiple Sequence Alignment Software Version 7: Improvements in Performance and Usability.” *Molecular Biology and Evolution* 30 (4): 772–80.

Katz, Paul S., and Phoenix D. Quinlan. 2019. “The Importance of Identified Neurons in Gastropod Molluscs to Neuroscience.” *Current Opinion in Neurobiology* 56 (June): 1–7.

Kawaguchi, Daichi, Takeshi Yoshimatsu, Katsuto Hozumi, and Yukiko Gotoh. 2008. “Selection of Differentiating Cells by Different Levels of Delta-like 1 among Neural Precursor Cells in the Developing Mouse Telencephalon.” *Development* 135 (23): 3849–58.

Kuehn, Emily, David S. Clausen, Ryan W. Null, Bria M. Metzger, Amy D. Willis, and B. Duygu Özpolat. 2021. “Segment Number Threshold Determines Juvenile Onset of Germline Cluster Expansion in Platynereis Dumerilii.” *Journal of Experimental Zoology. Part B, Molecular and Developmental Evolution*, November. https://doi.org/10.1002/jez.b.23100.

Lacin, Haluk, W. Ryan Williamson, Gwyneth M. Card, James B. Skeath, and James W. Truman.

2020. “Unc-4 Acts to Promote Neuronal Identity and Development of the Take-off Circuit in the Drosophila CNS.” *eLife* 9 (March). https://doi.org/10.7554/eLife.55007.
Lee, Kyung Eun, Jihae Seo, Jiheon Shin, Eun Hye Ji, Jiwon Roh, Joo Yeon Kim, Woong Sun, Jonas Muhr, Sanghyuk Lee, and Jaesang Kim. 2014. “Positive Feedback Loop between Sox2 and Sox6 Inhibits Neuronal Differentiation in the Developing Central Nervous System.” *Proceedings of the National Academy of Sciences of the United States of America* 111 (7): 2794–99.
Lein, Ed S., Michael J. Hawrylycz, Nancy Ao, Mikael Ayres, Amy Bensinger, Amy Bernard, Andrew F. Boe, et al. 2007. “Genome-Wide Atlas of Gene Expression in the Adult Mouse Brain.” *Nature* 445 (7124): 168–76.
Leonard, Janet L. 2000. *Identifiable Neurons in Invertebrates: From Invariant Cells to Dynamic Systems*. Verlag S. Karger.
Li, Lingling, Cristina Medina-Menéndez, Laura García-Corzo, Carmen M. Córdoba-Beldad, Alejandra C. Quiroga, Elena Calleja Barca, Valeriya Zinchuk, et al. 2022. “SoxD Genes Are Required for Adult Neural Stem Cell Activation.” *Cell Reports* 38 (5): 110313.
Lillvis, J. L., C. A. Gunaratne, and P. S. Katz. 2012. “Homology and Homoplasy of Swimming Behaviors and Neural Circuits in the Nudipleura (Mollusca, Gastropoda, Opisthobranchia).” *Proceedings of the*. http://www.pnas.org/content/109/Supplement_1/10669.short.
Lillvis, Joshua L., and Paul S. Katz. 2013. “Parallel Evolution of Serotonergic Neuromodulation Underlies Independent Evolution of Rhythmic Motor Behavior.” *The Journal of Neuroscience: The Official Journal of the Society for Neuroscience* 33 (6): 2709–17.
Linser, P. J., H. G. Trapido-Rosenthal, and E. Orona. 1997. “Glutamine Synthetase Is a Glial-Specific Marker in the Olfactory Regions of the Lobster (Panulirus Argus) Nervous System.” *Glia* 20 (4): 275–83.
MacManes, Matthew D. 2018. “The Oyster River Protocol: A Multi-Assembler and Kmer Approach for de Novo Transcriptome Assembly.” *PeerJ* 6 (August): e5428.
Manzanares, M., A. Locascio, and M. A. Nieto. 2001. “The Increasing Complexity of the Snail Gene Superfamily in Metazoan Evolution.” *Trends in Genetics: TIG* 17 (4): 178–81.
Marcinkiewicz, M., P. Touraine, and M. Chrétien. 1994. “Pan-Neuronal mRNA Expression of the Secretory Polypeptide 7B2.” *Neuroscience Letters* 177 (1-2): 91–94.
Martin, Emil, Vladimir Berka, Ah-Lim Tsai, and Ferid Murad. 2005. “Soluble Guanylyl Cyclase: The Nitric Oxide Receptor.” *Methods in Enzymology* 396: 478–92.
Matsuo, Ryota, Suguru Kobayashi, Arisa Furuta, Tomohiro Osugi, Toshio Takahashi, Honoo Satake, and Yuko Matsuo. 2020. “Distribution and Physiological Effect of Enterin Neuropeptides in the Olfactory Centers of the Terrestrial Slug Limax.” *Journal of Comparative Physiology. A, Neuroethology, Sensory, Neural, and Behavioral Physiology* 206 (3): 401–18.
Megalou, E. V., C. J. Brandon, and W. N. Frost. 2009. “Evidence That the Swim Afferent Neurons of Tritonia Diomedea Are Glutamatergic.” *The Biological Bulletin* 216 (2): 103–12.
Melsted, Páll, A. Sina Booeshaghi, Lauren Liu, Fan Gao, Lambda Lu, Kyung Hoi Joseph Min, Eduardo da Veiga Beltrame, Kristján Eldjárn Hjörleifsson, Jase Gehring, and Lior Pachter. 2021. “Modular, Efficient and Constant-Memory Single-Cell RNA-Seq Preprocessing.” *Nature Biotechnology* 39 (7): 813–18.
Moroz, L. L., and R. Gillette. 1996. “NADPH-Diaphorase Localization in the CNS and Peripheral Tissues of the Predatory Sea-Slug Pleurobranchaea Californica.” *The Journal of Comparative Neurology* 367 (4): 607–22.
Nakakura, Eric K., D. Neil Watkins, Kornel E. Schuebel, Virote Sriuranpong, Michael W. Borges, Barry D. Nelkin, and Douglas W. Ball. 2001. “Mammalian Scratch: A Neural-Specific Snail Family Transcriptional Repressor.” *Proceedings of the National Academy of Sciences* 98 (7): 4010–15.
Newcomb, James M., David J. Fickbohm, and Paul S. Katz. 2006. “Comparative Mapping of

Serotonin-Immunoreactive Neurons in the Central Nervous Systems of Nudibranch Molluscs." *The Journal of Comparative Neurology* 499 (3): 485–505.
Newcomb, James M., Akira Sakurai, Joshua L. Lillvis, Charuni A. Gunaratne, and Paul S. Katz. 2012. "Homology and Homoplasy of Swimming Behaviors and Neural Circuits in the Nudipleura (Mollusca, Gastropoda, Opisthobranchia)." *Proceedings of the National Academy of Sciences* 109 Suppl : 10669–76.
Newcomb, J. M., and W. H. Watson 3rd. 2001. "Identifiable Nitrergic Neurons in the Central Nervous System of the Nudibranch Melibe Leonina Localized with NADPH-Diaphorase Histochemistry and Nitric Oxide Synthase Immunoreactivity." *The Journal of Comparative Neurology* 437 (1): 70–78.
Nieto, M. Angela. 2002. "The Snail Superfamily of Zinc-Finger Transcription Factors." *Nature Reviews. Molecular Cell Biology* 3 (3): 155–66.
Nomaksteinsky, Marc, Stefan Kassabov, Zoubida Chettouh, Henri-Corto Stoeklé, Laure Bonnaud, Gilles Fortin, Eric R. Kandel, and Jean-François Brunet. 2013. "Ancient Origin of Somatic and Visceral Neurons." *BMC Biology* 11 (April): 53.
Oliver, G., A. Mailhos, R. Wehr, N. G. Copeland, N. A. Jenkins, and P. Gruss. 1995. "Six3, a Murine Homologue of the Sine Oculis Gene, Demarcates the Most Anterior Border of the Developing Neural Plate and Is Expressed during Eye Development." *Development* 121 (12): 4045–55.
Petersen, Kristen R., David A. Streett, Alida T. Gerritsen, Samuel S. Hunter, and Matthew L. Settles. 2015. "Super Deduper, Fast PCR Duplicate Detection in Fastq Files." In *Proceedings of the 6th ACM Conference on Bioinformatics, Computational Biology and Health Informatics*, 491–92. BCB '15. New York, NY, USA: Association for Computing Machinery.
Pflugrad, A., J. Y. Meir, T. M. Barnes, and D. M. Miller 3rd. 1997. "The Groucho-like Transcription Factor UNC-37 Functions with the Neural Specificity Gene Unc-4 to Govern Motor Neuron Identity in C. Elegans." *Development* 124 (9): 1699–1709.
Price, Morgan N., Paramvir S. Dehal, and Adam P. Arkin. 2010. "FastTree 2--Approximately Maximum-Likelihood Trees for Large Alignments." *PloS One* 5 (3): e9490.
Sakurai, Akira, and Paul S. Katz. 2017. "Artificial Synaptic Rewiring Demonstrates That Distinct Neural Circuit Configurations Underlie Homologous Behaviors." *Current Biology: CB* 27 (12): 1721–34.e3.
Santos, Paula dos, Günther Gehlen, M. Cristina Faccioni-Heuser, Denise M. Zancan, and Matilde Achaval. 2002. "Distribution of Glial Cells in the Central Nervous System of the Pulmonate Snail Megalobulimus Oblongus Identified by Means of a Glial Fibrillary Acidic Protein Marker." *Acta Zoologica* 83 (4): 345–51.
Schultz, L. M., and G. A. Clark. 1997. "GABA-Induced Synaptic Facilitation at Type B to A Photoreceptor Connections in Hermissenda." *Brain Research Bulletin* 42 (5): 377–83.
Schulz, Marcel H., Daniel R. Zerbino, Martin Vingron, and Ewan Birney. 2012. "Oases: Robust de Novo RNA-seq Assembly across the Dynamic Range of Expression Levels." *Bioinformatics* 28 (8): 1086–92.
Seidel, B., W. Dong, D. Savaria, M. Zheng, J. E. Pintar, and R. Day. 1998. "Neuroendocrine Protein 7B2 Is Essential for Proteolytic Conversion and Activation of Proprotein Convertase 2 in Vivo." *DNA and Cell Biology* 17 (12): 1017–29.
Seimiya, M., and W. J. Gehring. 2000. "The Drosophila Homeobox Gene Optix Is Capable of Inducing Ectopic Eyes by an Eyeless-Independent Mechanism." *Development* 127 (9): 1879–86.
Seo, H. C., Drivenes, S. Ellingsen, and A. Fjose. 1998. "Expression of Two Zebrafish Homologues of the Murine Six3 Gene Demarcates the Initial Eye Primordia." *Mechanisms of Development* 73 (1): 45–57.
Shi, Xiaowei, Lingling Wang, Zhi Zhou, Rui Liu, Yunchen Li, and Linsheng Song. 2014.

"Acetylcholine Modulates the Immune Response in Zhikong Scallop Chlamys Farreri." *Fish & Shellfish Immunology* 38 (1): 204–10.
Sinigaglia, Chiara, Daniel Thiel, Andreas Hejnol, Evelyn Houliston, and Lucas Leclère. 2018. "A Safer, Urea-Based in Situ Hybridization Method Improves Detection of Gene Expression in Diverse Animal Species." *Developmental Biology* 434 (1): 15–23.
Smith-Unna, Richard, Chris Boursnell, Rob Patro, Julian M. Hibberd, and Steven Kelly. 2016. "TransRate: Reference-Free Quality Assessment of de Novo Transcriptome Assemblies." *Genome Research* 26 (8): 1134–44.
Songco-Casey, Jeremea O., Gabrielle C. Coffing, Denise M. Piscopo, Judit R. Pungor, Andrew D. Kern, Adam C. Miller, and Cristopher M. Niell. 2022. "Cell Types and Molecular Architecture of the Octopus Bimaculoides Visual System." *Current Biology: CB* 32 (23): 5031–44.e4.
Spijker, S., A. B. Smit, H. E. Sharp-Baker, R. Van Elk, E. R. Van Kesteren, J. Van Minnen, A. Kurosky, and W. P. Geraerts. 1999. "Family of Prohormone Convertases in Lymnaea: Characterization of Two Alternatively Spliced Furin-like Transcripts and Cell-Specific Regulation of Their Expression." *Journal of Neurobiology* 41 (3): 399–413.
Storch, V., and U. Welsch. 1969. "Über Bau Und Funktion Der Nudibranchier-Rhinophoren." *Cell and Tissue Research*.
Stump, Gila, André Durrer, Anne-Laurence Klein, Simone Lütolf, Ueli Suter, and Verdon Taylor. 2002. "Notch1 and Its Ligands Delta-like and Jagged Are Expressed and Active in Distinct Cell Populations in the Postnatal Mouse Brain." *Mechanisms of Development* 114 (1-2): 153–59.
Styfhals, Ruth, Grygoriy Zolotarov, Gert Hulselmans, Katina I. Spanier, Suresh Poovathingal, Ali M. Elagoz, Seppe De Winter, et al. 2022. "Cell Type Diversity in a Developing Octopus Brain." *Nature Communications* 13 (1): 7392.
Sun, Woong, Hiroshi Funakoshi, and Toshikazu Nakamura. 2002. "Localization and Functional Role of Hepatocyte Growth Factor (HGF) and Its Receptor c-Met in the Rat Developing Cerebral Cortex." *Brain Research. Molecular Brain Research* 103 (1-2): 36–48.
Thiel, Daniel, Luis A. Yañez-Guerra, Mirita Franz-Wachtel, Andreas Hejnol, and Gáspár Jékely. 2021. "Nemertean, Brachiopod, and Phoronid Neuropeptidomics Reveals Ancestral Spiralian Signaling Systems." *Molecular Biology and Evolution* 38 (11): 4847–66.
Veenstra, Jan A. 2010. "Neurohormones and Neuropeptides Encoded by the Genome of Lottia Gigantea, with Reference to Other Mollusks and Insects." *General and Comparative Endocrinology* 167 (1): 86–103.
Vergara, Hernando Martínez, Paola Yanina Bertucci, Peter Hantz, Maria Antonietta Tosches, Kaia Achim, Pavel Vopalensky, and Detlev Arendt. 2017. "Whole-Organism Cellular Gene-Expression Atlas Reveals Conserved Cell Types in the Ventral Nerve Cord of Platynereis Dumerilii." *Proceedings of the National Academy of Sciences of the United States of America* 114 (23): 5878–85.
Walters, E. T., M. Bodnarova, and A. J. Billy. 2004. "Somatotopic Organization and Functional Properties of Mechanosensory Neurons Expressing sensorin‐A mRNA in Aplysia Californica." *Journal of*. https://onlinelibrary.wiley.com/doi/abs/10.1002/cne.20042?casa_token=XLFrPzLYr2UAAAAA:xgWzsLz0jxTjVos9PYOm0cPNrqPAW3wiFcD_I6ZTb8Ep_mDFcyYUdbGIUx2mdYCNr6zgf42jbxl1wXA.
Watkins, Kelsi L. 2022. "Chemosensory Receptors in Berghia Stephanieae: Bioinformatics and Localization." University of Massachusetts Amherst. https://doi.org/10.7275/31053258.
Wertz, Adrian, Wolfgang Rössler, Malu Obermayer, and Ulf Bickmeyer. 2006. "Functional Neuroanatomy of the Rhinophore of Aplysia Punctata." *Frontiers in Zoology* 3 (April): 6.
Whitesel, Carl Arthur. 2021. "Studying the Central and Peripheral Nervous Systems in Larval and Juvenile Berghia Stephanieae." UC San Diego.

https://escholarship.org/uc/item/8k07146f.
Williams, Elizabeth A., Csaba Verasztó, Sanja Jasek, Markus Conzelmann, Réza Shahidi, Philipp Bauknecht, Olivier Mirabeau, and Gáspár Jékely. 2017. “Synaptic and Peptidergic Connectome of a Neurosecretory Center in the Annelid Brain.” *eLife* 6 (December). https://doi.org/10.7554/eLife.26349.
Xie, Yinlong, Gengxiong Wu, Jingbo Tang, Ruibang Luo, Jordan Patterson, Shanlin Liu, Weihua Huang, et al. 2014. “SOAPdenovo-Trans: De Novo Transcriptome Assembly with Short RNA-Seq Reads.” *Bioinformatics* 30 (12): 1660–66.
Xiong, W. C., H. Okano, N. H. Patel, J. A. Blendy, and C. Montell. 1994. “Repo Encodes a Glial-Specific Homeo Domain Protein Required in the Drosophila Nervous System.” *Genes & Development* 8 (8): 981–94.
Yeoman, M. S., A. W. Pieneman, G. P. Ferguson, A. Ter Maat, and P. R. Benjamin. 1994. “Modulatory Role for the Serotonergic Cerebral Giant Cells in the Feeding System of the Snail, Lymnaea. I. Fine Wire Recording in the Intact Animal and Pharmacology.” *Journal of Neurophysiology* 72 (3): 1357–71.
Zappia, Luke, and Alicia Oshlack. 2018. “Clustering Trees: A Visualization for Evaluating Clusterings at Multiple Resolutions.” *GigaScience* 7 (7). https://doi.org/10.1093/gigascience/giy083.
Zhang, Han, Marcy Wainwright, John H. Byrne, and Leonard J. Cleary. 2003. “Quantitation of Contacts among Sensory, Motor, and Serotonergic Neurons in the Pedal Ganglion of Aplysia.” *Learning & Memory* 10 (5): 387–93.